Master's Thesis of Landscape Architecture

항만지역 배후 주거단지 대기질 개선을 위한 효율적 그린인프라 적용
: 전산유체역학을 활용한 수치분석

Efficient Application of Green Infrastructure for Improving Air Quality in Residential Complexes behind Port Area
: Numerical Analysis using Computational Fluid Dynamics

August 2023

Graduate School of Seoul National University

Department of Landscape Architecture and Rural
Systems Engineering, Landscape Architecture Major

Seunghun Baek

Efficient Application of Green Infrastructure for Improving Air Quality in Residential Complexes behind Port Area
: Numerical Analysis using Computational Fluid Dynamics

Under the Direction of Advisor, Prof. Junsuk Kang

Submitting a master's thesis of
Landscape Architecture

August 2023

Graduate School of Seoul National University

Department of Landscape Architecture and Rural Systems Engineering, Landscape Architecture Major

Seunghun Baek (Sign)

Confirming the master's thesis
Written by Seunghun Baek

May 2023

Chair ______________________ **(Seal)**

Vice Chair ______________________ **(Seal)**

Examiner ______________________ **(Seal)**

Abstract

Efficient Application of Green Infrastructure for Improving Air Quality in Residential Complexes behind Port Area : Numerical Analysis using Computational Fluid Dynamics

Seunghun Baek
Master's Course in Landscape Architecture
Graduate School, Seoul National University
Supervised by Professor Junsuk Kang

Korea is one of the countries with serious air pollution among OECD member countries. In particular, in port areas, large amounts of pollutants are discharged due to a large volume of maritime traffic, which accounts for a high proportion of air pollution in the area. Currently, policies to improve air quality mainly focus on regulating emission sources themselves. However, when examining the fluctuation trend of fine dust concentrations in major cities in Korea, the effectiveness of emission source regulation policies is being questioned, indicating the need for spatial management measures.

This study focused on Busan Port, which handles more than half of the maritime traffic in the largest port city in Korea, and is expected to have poor air quality. More specifically, the study targeted the densely populated residential areas behind the port in Busan New Port. It was determined that a spatial measure is necessary to improve air quality in the Busan New Port area, moving away from the conventional approach of only regulating emission sources. In this study, green infrastructure, which is known to reduce various types of disasters and hazards, was utilized as a measure.

The objective of this study is to quantitatively demonstrate the effectiveness of introducing green infrastructure in improving air quality in the residential areas behind the port in Busan, which is expected to have poor air quality due to processing more than half of the marine traffic in the city. Specifically, the study focused on densely populated residential areas within Busan New Port. To achieve the goal of improving air quality in the port area of Busan, it was deemed necessary to move beyond the conventional approach of regulating emission sources and adopt spatial strategies. In this study, various forms of green infrastructure were simulated in the target area, and computational fluid dynamics were utilized to quantitatively evaluate their effects and provide an optimal placement plan. In order to use the CFD model, a correlation analysis was conducted between field data such as air quality observation stations and meteorological information data, and it showed a correlation coefficient of 0.7 or higher, indicating that the data was reliable. The green infrastructure used in this study considered the vegetation form in the target area and utilized trees and shrubs, and simulations were conducted for a total of 30 cases by combining spacing and arrangement of green infrastructures.

This study introduces green infrastructure as a spatial improvement strategy for the residential areas behind the port in the harbor area where fine dust pollution is high, but management measures are insufficient, and suggests a placement plan. This study is expected to serve as a fundamental basis for spatial improvement strategies for air quality in the port area in the future.

Keywords : Computational fluid dynamics, Green Infrastructure, Air quality, Port area, Fine dust

Student Number : 2021-20044

Table of Contents

List of Tables

List of Figures

Chapter 1. Introduction

1.1 Background

Although it has been deflected from our attention due to the COVID-19 pandemic, which has been a global issue from 2020 to the present, Particulate air pollution, especially the types with aerodynamic diameter of less than 2.5 µm (PM2.5), is a matter of public concern, because it is known to exacerbate a wide range of respiratory and vascular illnesses (Brunekreef & Holgate, 2002). According to the '2019 World Air Quality Report', Korea showed a high enough level to rank first among OECD member countries in the concentration of ultrafine dust pollution (AirVisual, 2019). 2020 brought unexpected reductions in air pollution due to reduced human activity due to the pandemic, but the recent resumption of activity is expected to increase air pollution again.

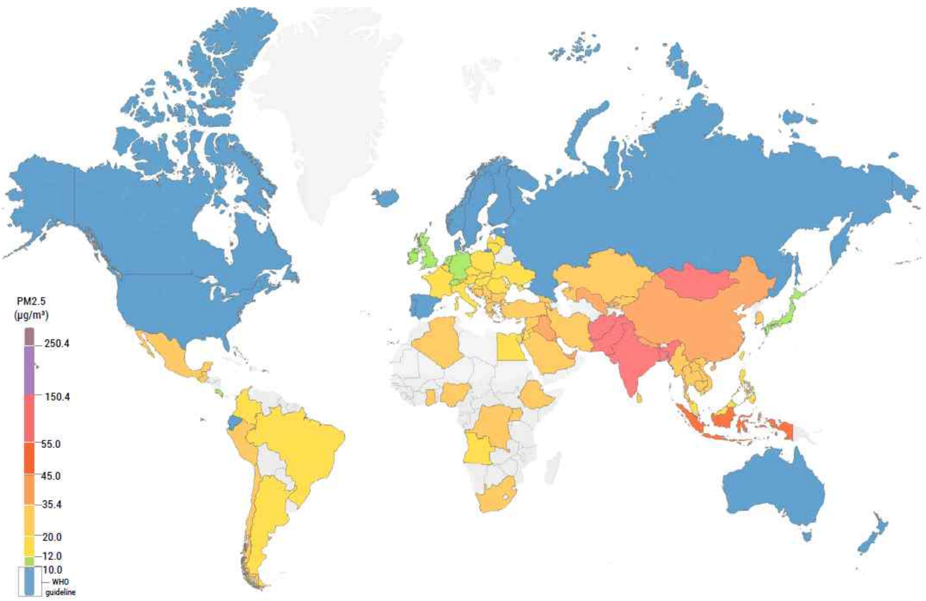

Fig. 1 2019 global PM2.5 concentration (Airvisual, 2019)

Maritime transportation through ships accounts for 85% of total global trade, and in Korea's maritime traffic accounts for 99.7%. In port area with a lot of maritime traffic, various types of air pollutants are detected from sources including ships. Of Korea's air pollutant emissions, the amount of fine dust generated from the marine section accounts for 9.6% of the country, and 51.4% in Busan alone, which is a very serious level (Han, 2017). According to the World Shipping Coucil's data on the maritime traffic for each city in the world, Busan is the 7th largest city in the world as of 2020. It was similar to cities including Shanghai in China, and it can be seen that it is higher than that of Incheon, Gwangyang, and Ulsan, which are major port area of Republic of Korea.

Table. 1 Maritime traffic of major port

(Million TEU)

No.	Volume 2016	Volume 2017	Volume 2018	Volume 2019	Volume 2020
1	Shanghai (37.13)	Shanghai (40.23)	Shanghai (42.01)	Shanghai (43.30)	Shanghai (43.50)
2	Singapore (30.9)	Singapore (33.67)	Singapore (36.60)	Singapore (37.20)	Singapore (36.60)
3	Shenzhen (23.97)	Shenzhen (25.21)	Shenzhen (27.74)	Ningbo-Zhoushan (27.49)	Ningbo-Zhoushan (28.72)
4	Ningbo-Zhoushan (21.6)	Ningbo-Zhoushan (24.61)	Ningbo-Zhoushan (26.35)	Shenzhen (25.77)	Shenzhen (26.55)
5	Busan (19.85)	Busan (20.49)	Guangzhou (21.87)	Guangzhou (23.23)	Guangzhou (23.19)
6	Guangzhou (18.85)	Guangzhou (20.37)	Busan (21.66)	Busan (21.99)	Qingdao (22.00)
7	Qingdao (18.01)	Qingdao (18.30)	Qingdao (18.26)	Qingdao (21.01)	Busan (21.59)

Comparing the drift in the proportion of maritime traffic between the North Port and the New Port, which account for more than 95% of Busan, over the past 7 years, the North Port accounted for around 35% each year. New ports accounted for more than 60% every year, showing that they accounted for most of Busan's maritime traffic. Busan New Port opened in 2006 and currently has 25 berths and plans to gradually expand the facilities to 57 berths by 2040, so the amount of air pollutants to be emitted is expected to increase.

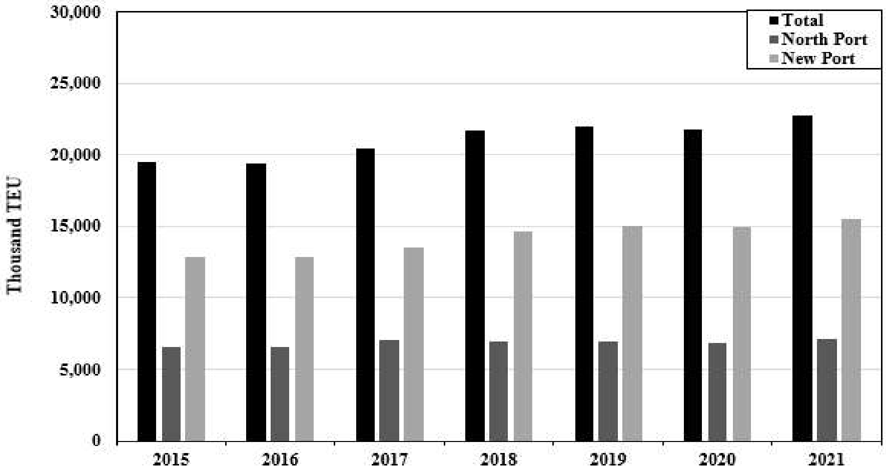

Fig. 2 Comparison of maritime traffic in Busan

As the air quality deteriorated due to the increase of maritime traffic in the port area, the government announced the ‘Comprehensive Plan for Air Quality Improvement in Port Areas’ (Ministry of Oceans and Fisheries, 2021). Policies are mainly regulating ships, which are emission sources, and there are insufficient specific measures to reduce damage to nearby residents. The metropolitan area, such as Seoul, which is an inland area, also introduced policies focusing on emission source control, starting with the first basic plan for air environment management in the metropolitan area in 2005. Looking at the trend of fluctuations in the amount of fine dust by year in Seoul, it showed a gradually decreasing pattern after the policy was introduced, but it can be seen that the correlation between the emission source and the pollution concentration is decreasing around 2012. This suggests that a policy to simply regulate emission sources is not enough, and port areas will be similar. Accordingly, it is necessary to quantitatively analyze the impact that a source that emits a large amount of pollutants may have on the surrounding area and suggest alternatives in parallel with the emission source regulation and spatial management response plan.

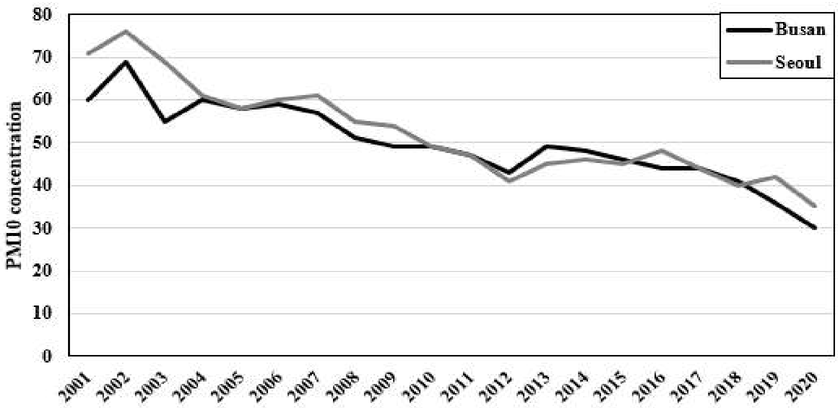

Fig. 3 Fluctuation of fine dust concentration in Seoul & Busan

One of the methods to improve air quality in terms of urban spatial structure is green infrastructure(GI) such as street trees and parks. GI has the function of absorbing and adsorbing fine dust through the outer surface and pores. It also promotes atmospheric circulation by creating a curved surface in the urban space with the building. In order to analyze how pollutants are distributed in the external space, a method for analyzing air flow is required. Common methods for analyzing atmospheric flow include field experiments and wind tunnel experiments. However, there is a limit to considering these variables in an experimental method because the distribution of air pollutants is heterogeneous in urban space due to the non-uniform wind flow due to the large number of buildings and irregular sections of solar radiation. With the recent development of hardware and software, computational fluid dynamics, which supplements the above-mentioned limitations and can consider various situations as well as fragmentary phenomena, is being actively used. This is attracting attention as a method of analyzing atmospheric flow because it allows quantitative analysis including various environmental variables by dividing space into mesh and storing physical properties to compute physical interactions between mesh.

1.2. Objectives

The objective of this study is to derive an optimal design for the introduction of green infrastructure as a mitigation measure for reducing a significant amount of air pollutants emitted from ships due to a large amount of water flow into Busan New Port, where the air quality is poor. Green infrastructure is one of the frequently adopted mitigation measures to respond to various disasters and hazards in our surroundings, such as air pollution and heatwaves. In particular, green infrastructure is known to be effective in improving air quality by promoting the circulation of air flow in the city like a wind path and adsorbing air pollutants through its leaf surface. Therefore, while green infrastructure is actively being introduced as a policy decision by policymakers, there is a lack of quantitative evidence that can serve as a standard for its actual introduction. In this study, we aim to present the optimal green infrastructure deployment plan using computational fluid dynamics, which is difficult to determine the effectiveness of through various experiments, and provide quantitative effects.

1.3 Scope and Flow

This study is mainly composed of four chapters: background, previous research review, methodology, and numerical analysis (fig. 1). In this chapter, as the background of the study, the target area of this study was explained based on the air quality risk and statistical data of the port area, and the objective of this study was explained. The literature review was divided into three parts: 1) Air quality analysis using CFD, the main method of this study, 2) Green infrastructure and reduction effects within CFD, 3) Initial CFD A method of calculating fine dust emissions to be applied as a condition. Methodology includes a series of processes to achieve the objective of the research. Build a model framework using geospatial and building information, and build a basic model by calculating initial emissions based on data that includes information such as ships. For the verification of the model, the CFD analysis result of the model is compared with the environmental information actually measured in the target area, Busan New Port. Based on the verified model, vulnerable residential complexes are selected within the Busan New Port and the green infrastructure to be introduced as an alternative to fine dust mitigation in the area is modeled. Finally, in order to select an optimal design plan and derive its quantitative effect, numerical analysis is performed by classifying scenarios according to the arrangement of green and grey infrastructure.

Fig. 4 Research scope and flow

Chapter 2. Literature Review

2.1 Air quality analysis using CFD

The Computational Fluid Dynamics model obtains quantitative results by solving the advection and dispersion equations of air pollutants such as PM2.5 and PM10 in the flow field of the target area obtained by using the Navier-Stokes equation. Urban areas, where various buildings and other infrastructure are densely concentrated, have many limitations in predicting flow and microclimate characteristics due to their complex structure. Under the premise that the CFD model has a high correlation with field, it provides information to researchers and decision makers through simulation of various environmental variables such as wind direction and wind speed, unlike field measurement, which only considers fragmentary situations.

The CFD model provides a wider range for implementing different turbulence models and solution methods. In general, turbulence is explicitly resolved in the Direct Numeric Simulation (DNS) model, while in the Reynolds Averaged Naiver-Stokes (RANS) and Large Eddy Simulations (LEM) models, it is parameterized using different concepts. Toparlar et al, 2017 has investigated studies using CFD on urban microclimate up to 2015. As a result, 96% of the studies used the RANS model to solve the Navier-Stokes governing equation, 2.8% used LES, and the rest used both. Although the LES simulation is known to be accurate (Jeanjean et al. 2017), due to high computational requirements and lack of best practice guidelines (Toparal et al. 2017) The frequency of use was low. When categorizing studies according to geographic scale, of the 177 studies reported, 30% exhibited regional scales, 30% urban scales, 15% regional scales, and 15% street scales (Kadaverugu et al. 2019).

In a recent study, in addition to air quality analysis, research on how quantitatively improved by introducing green infrastructure as a solution for outdoor air quality improvement was being conducted. Green infrastructure is known to act as a defense wall to block pollutants in the city, and to reduce the amount of pollutants by being absorbed by crown with leaves. Gallagher et al. (2015) found that tree species, crown size, porosity, leaf area density, height, and tree-building distance influence particle dispersion. Jeanjean, Monks, & Leigh (2016) used OpenFOAM software to discuss the effects of trees and grass on the reduction of PM2.5 caused by traffic emission at the city scale. It was found that the aerodynamic effect was superior to the deposition effect, and when the wind speed was more than 2 m/s, the tree showed a beneficial effect. In the field of air quality analysis, there have been studies specifically focusing on pedestrians as the actual end-users. Grimke & Blocked (2014) found the effects of street trees on flow and dispersion at pedestrian heights in general urban spaces using CFD software FLUENT.

In addition, the analysis was conducted considering coupling effects of building and tree (Hong, 2017). RANS model and the revised generalized drift flux model was used to discuss the dispersion effect of PM2.5 according to different building-tree arrangements in the housing block.

The simulation models go through a validation process to evaluate whether this is actually a reasonable method. Model performance is typically assessed by calculating statistical metrics such as correlation coefficients, normalized mean bias, mean fractional error and bias, and normalized mean square error between modeled and observed environmental variables (Zhong et al. 2016).

2.2 Implementation of Green Infrastructures

In related studies using CFD, the fine dust reduction effect of green infrastructure has been largely analyzed using wind tunnel experiments and numerical models. The wind tunnel experiment has the advantage that it can be simulated similarly to the real one, but it has the disadvantage of showing only the result of the integrated effect, without distinguishing what effect the reduction is due to. However, by using a numerical model, it is possible to analyze the contribution level of the effects of reducing fine dust and quantitative numerical values. Although it is not an accessible method because the software is expensive, it is a suitable method for the study of various physical flow and dispersion processes in complex geometry such as cities.

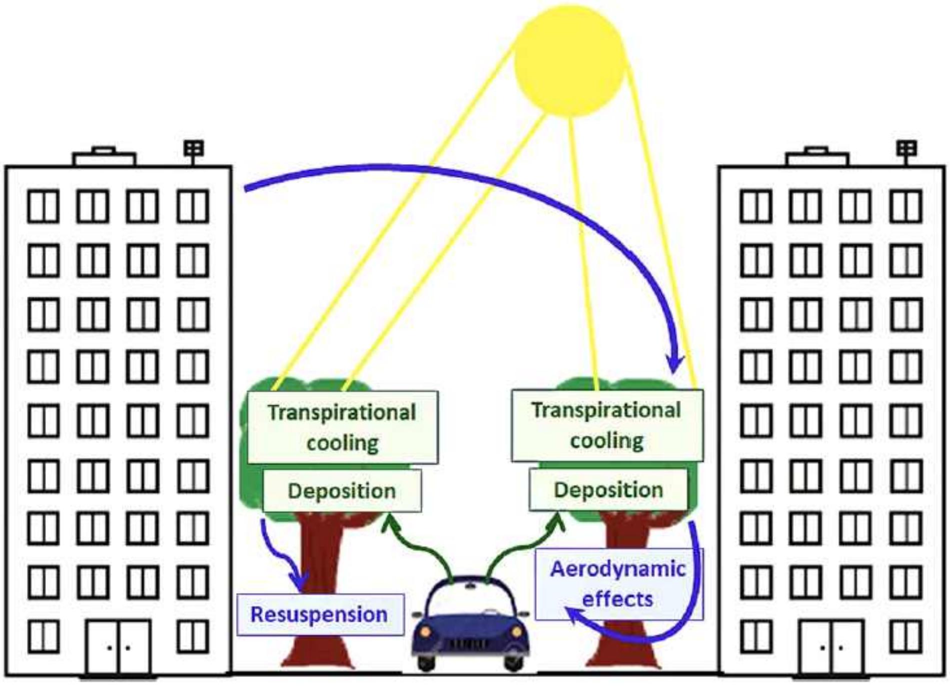

Fig. 5 Effects of greenInfrastructures related to fine dust in the CFD model (Buccolieri et al, 2018)

There are three main effects of green infrastructure and street trees, which are currently being applied in research on fine dust using CFD. 1) aerodynamic effect to weaken the diffusion of fine dust by obstructing air flow around trees, 2) deposition effect to remove fine dust through the leaves in the canopy layer of trees, 3) resuspension effect of fine dust captured on the surface of trees.

2.2.1 Aerodynamic effect

In most studies, the porous vegetation approach has been used to simulate the aerodynamic effects of green infrastructure. For this purpose, the standard fluid flow equations were supplemented with momentum source (sink) terms. Recent studies using computational fluid dynamics (CFD) have parameterized the drag force between leaves and the atmosphere for each grid. Leaf area density (LAD) $[m^2 m^{-3}]$, which represents the leaf area per unit volume, was used, and the sink of momentum term was added to each momentum equation. as:

$$S_{ui} = -\rho LAD C_d U ui \quad [Pa\, m^{-1}] \tag{1}$$

where ρ is the air density $[kg\, m^{-3}]$, C_d is the sectional drag for vegetation (dimensionless), U is the wind speed $[m\, s^{-1}]$, ui is the wind velocity component $[m\, s^{-1}]$. The value of C_d used in Eq. (1) has a variation in different studies. Table. 2 represents the values of C_d used in previous studies.

In addition, vegaetation has a effect of modifying the mean flow motion of the surrounding air. Vegetation alters the flow pattern and creates wake turbulence in its vicinity. However, the turbulence generated by the wake is smaller in length scale compared to the turbulence generated by the shear of the incoming flow. As a result, this wake turbulence experiences a fast dissipation process. This is parameterized through source and sink terms for turbulent kinetic energy (k) and turbulent dissipation rate (ε) in the turbulence equations as:

$$S_k = \rho LADC_d(\beta_p U^3 - \beta_d Uk) \ [kgm^{-1}s^{-3}] \tag{2}$$

$$S_\epsilon = \rho LADC_d(C_{\epsilon 4}\beta_p \frac{\epsilon}{k} U^3 - C_{\epsilon 5}\beta_d U\epsilon) \ [kgm^{-1}s^{-4}] \tag{3}$$

where β_p is the fraction of mean kinetic energy converted into turbulent kinetic energy and it takes value between 0 and 1, β_d is coefficient for short circuiting of the turbulence (dimensionless). $C_{\epsilon 4}$ and $C_{\epsilon 5}$ are constants for the model. Table. 3, Table. 4 represent the values of β_p, β_d, $C_{\epsilon 4}$ and $C_{\epsilon 5}$ used in previous studies.

Table. 2 Values of sectional drag coefficient used in CFD simulations (Buccolieri et al, 2018)

Additional Term	C_d	References
$S_{ui} = -\rho LADC_d Uui$	0.1-0.3	Vrancks et al. (2015)
	0.2	Gromke et al. (2015), Santiago et al. (2013)
	0.25	Jeanjean et al. (2015)

Table. 3 Values of β_p, β_d, used in CFD simulations (Buccolieri et al, 2018)

Additional Term	Value	References
$S_k = \rho LADC_d(\beta_p U^3 - \beta_d Uk)$	β_p=1 β_d=4	Green (1992), Liu et al. (1996), Amorim et al. (2013), Salim et al. (2015)
	β_p=1 β_d=3	Hong et al. (2018)

Table. 4 Values of $C_{\epsilon 4}$, $C_{\epsilon 5}$ used in CFD simulations (Buccolieri et al, 2018)

Additional Term	Value	References
$S_\epsilon = \rho LAD C_d (C_{\epsilon 4}\beta_p \frac{\epsilon}{k} U^3 - C_{\epsilon 5}\beta_d U\epsilon)$	$C_{\epsilon 4}$=1.5 $C_{\epsilon 5}$=1.5	Green (1992), Katul et al. (2004), Amorim et al. (2013), Hong et al. (2018)
	$C_{\epsilon 4}$=1.5 $C_{\epsilon 5}$=0.6	Liu et al. (1996)

2.2.2 Deposition effect

In addition to the aerodynamic effect, it reduces the concentration of fine dust in the air through the deposition of fine dust on the leaves of trees. This is implemented as a volumetric sink term in the transport equation:

$$S_d = -LAD V_d C(x,y,z)\ [kg m^{-3} s^{-1}] \tag{4}$$

where V_d is the deposition velocity of target atmospheric substance $[m s^{-1}]$, C is the pollutant concentration of atmospheric substance $[kg m^{-3}]$. This additional term is proportional to the LAD, V_d and pollutant concentration in each mesh. Table. 5 represents the values of V_d used in previous studies.

Table. 5 Values of deposition velocities used in CFD simulations (Buccolieri et al, 2018)

Additional Term	V_d	References
$S_d = -LAD V_d C(x,y,z)$	0.2-1 (PM10)	Vos et al. (2013)
	0.5-5 (PM10)	Vrancks et al. (2015)
	0.64 (PM2.5)	Jeanjean et al. (2015), (2017)
	0.5-3 (NOx)	Santiago et al. (2017b)
	4.58 (PM2.5)	Hong et al. (2018)

2.2.3 Resuspension effect

The resuspension effect takes into account that fine dust deposited on trees is released back into the atmosphere by the wind. According to previous studies, (Nowak et al. 2013) showed that PM2.5 resuspended from a minimum of 4.5% to a maximum of 12% from the leaves. This is implemented as a volumetric source term in the transport equation.

$$S_r = LADV_r C_{\sin k}(x,y,z)\ [kgm^{-3}s^{-1}] \tag{5}$$

S_r : Volumetric source

V_r : Resuspension velocity of particle $[ms^{-1}]$

$C_{\sin k}$: Particle concentration $[kgm^{-3}]$

The LAD values used in the Eq. (1), (2), (3) can be summarized in the following table.

Table. 6 Values of leaf area density used in CFD simulations (Buccolieri et al, 2018)

Leaf area density LAD	References
0.7 (tree) 2-5 (hedge)	Vos et al. (2013)
0.55-2	Gromke et al. (2015)
1.6-4	Vrancks et al. (2015)
1-1.6	Jeanjean et al. (2015)
0.1-0.5	Santiago et al. (2017b)
2.3	Hong et al. (2018)

2.3 Calculation of Air Pollutant Emissions

According to the National Fine Dust Information Center (2019) of the Ministry of Environment, ships are classified as non-road mobile pollution sources in the air pollutant classification system. The air pollutant emission calculation part from non-road mobile pollution sources is the part that calculates the air pollutant emissions from engines essential for operating ship. If the types of ship are further subdivided, they can be divided into passenger ships, cargo ships, fishing ships, and leisure ships. In the case of Busan New Port, the subject of this study, since it is a port that handles a large amount of cargo, the main types of ships entering and departing are cargo ships. The method of calculating air pollutant emissions from cargo ships is as follows.

The method of calculating air pollutant emissions of cargo ships that is followed in Korea calculates the emissions by dividing the arrival and departure process into three processes: 1) anchoring mode 2) berthing mode 3) operating mode. Anchoring mode refers to a state in which a ship stops sailing with its anchor at the bottom of the sea at sea, and calculates the amount of air pollutant emissions generated while a cargo ship is anchored. The berthing mode is to calculate the pollutant emissions generated while moving the pilotage distance, which is the distance from anchorage to the berthing facility of the pier. The operation mode is a section that calculates air pollutants emitted by cargo ships while sailing on the sea. Although it is possible to calculate air pollutant emissions from cargo ships through individual fuel consumption, the fuel consumption estimation equation is used because data is difficult to obtain :

$$E_{i,j} = F_j \times EF_i \tag{6}$$

$E_{i,j}$ is the air pollutant i emission of cargo ship j $[kg/yr]$, F_j is the fuel consumption of cargo ship j [, and EF_i is the combined emission factor of air pollutant i$[kg/$.

- Anchoring mode

Estimation of fuel consumption in anchoring mode utilizes the log of arrival and departure by gross tonage, anchoring time, and fuel consumption coefficient :

$$F_{wj} = A_{wj} \times SFOC \times 0.79 \times 0.2 \tag{7}$$

F_{wj} is the fuel consumption of the w ton cargo ship j in anchoring mode[, A_{wj} is the number of arrivals of the w ton cargo ship j, and SFOC is the fuel consumption factor at maximum output[. The fuel consumption factor used to estimate the fuel consumption in anchoring mode follows the standards of the European Environment Agency (EEA). This estimates the average daily fuel consumption by ship type and gross tonage. Since the fuel consumption factor calculation method shown in the table is based on the maximum output, the fuel consumption in anchoring mode is assumed to be 20% of the maximum output. In the case of the average number of anchoring days, 0.79 days are applied per one time, which is the result of analysis of 560 vessels that entered Ulsan Port in January and December 2011. (Han, 2021) calculated the emissions by correcting the average number of anchoring days to 0.99 days through analysis based on data from 2015 to 2016 in and out of Busan New Port.

Table. 7 Fuel consumption by ship type & gross tonage (EEA, 1999)

Type	Average fuel consumption	Fuel consumption by Gross Tonage
Solid bulk	33.8	20.186 + 0.00049*GT
liquid bulk	41.1	14.865 + 0.00079*GT
General cargo	21.3	9.8197 + 0.00143*GT
Container	65.9	8.0552 + 0.00235*GT
Passenger/Ro-Ro/Cargo	32.3	12.834 + 0.00156*GT
Passenger	70.2	16.904 + 0.00049*GT
High speed ferry	80.4	39.483 + 0.00972*GT
Inland cargo	21.3	9.8197 + 0.00143*GT
Sail ships	3.4	0.4268 + 0.00100*GT
Tugs	14.4	5.5651 + 0.01048*GT
Fishing	5.5	1.9387 + 0.00091*GT
Other ships	26.4	9.7126 + 0.00091*GT
All ships	32.8	16.263 + 0.001*GT

- berthing mode

Estimation of fuel consumption in berthing mode uses pilot distance (anchorage-pier berthing facility) and fuel economy data, and the equation is as follows :

$$F_j = A_{wj} \times Z_{wj} \times M_w^{-1} \tag{8}$$

F_{wj} is the fuel consumption of w ton cargo ship j when berthing$[k\ell]$, A_{wj} is the number of arrivals and departures of w ton cargo ship j, Z_{wj} is the pilot distance of w ton cargo ship j$[km]$, and M_w is the fuel economy value of w ton cargo ship j$[km/k\ell]$.

- operating mode

Fuel consumption in operating mode is estimated based on the arrival and departure times of individual ships and ship specification information. The engine load factor in operating mode is calculated assuming 80% of the maximum output suggested in EEA, 2019.

$$F_j = P_j \times SFOC \times 0.8 \times H_j \times 10^{-6} \tag{9}$$

F_j is the fuel consumption of cargo ship j during operating[, P_j is the engine power of cargo ship j[kW], and c is the operating time of cargo ship j[hr].

Chapter 3. Methodology

3.1 Geometry modelling

3.1.1 Topography

In order to increase the accuracy of fine dust analysis using CFD, more sophisticated shape modeling is essential. In this study, a model was built using Rhino3D, a 3D CAD application software based on NURBS mathematical model, and Grasshopper 3D, a graphic algorithm editor, which can construct sophisticated shapes in a relatively short time. The digital topographic map CAD file provided as an open source from the national spatial information portal operated by the Ministry of Land, Infrastructure and Transport was used to build the model. To construct the topography, the contour layer of the digital topographic map was used, and the range was set to a radius of 3 km centered on the residential complex. In order to make the curves of the contour layer into a single surface, points were extracted in units of 50 m through the Grasshopper algorithm, and the algorithm was configured to connect nearby points.

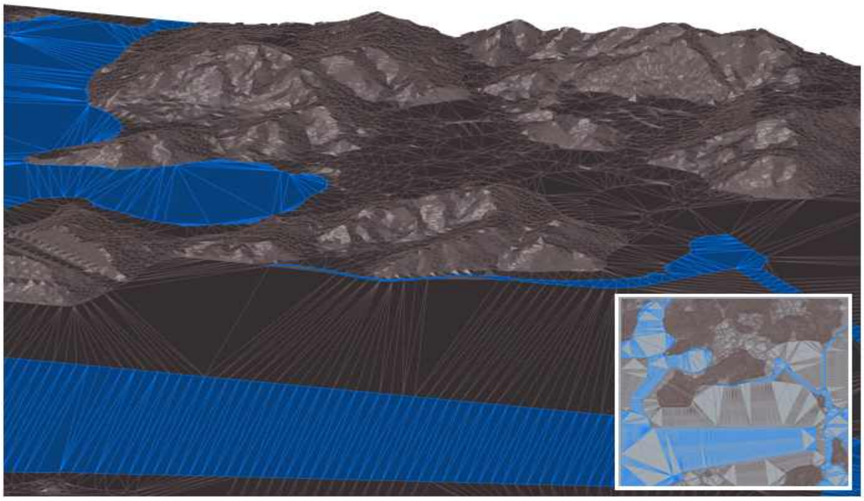

Fig. 6 Topography model using Rhino 3D

3.1.2. Grey Infrastructure

Grey infrastructure included within the model range of 6km x 6km includes residential buildings (apartments), other buildings. The number of geay infrastructure is about 4000, and it must be modeled so that it can be attached to the constructed topography. Although it is possible to model each grey infrastructure, it takes a lot of time, so Grasshopper and NGIMap, a numerical map application software of the Ministry of Land, Infrastructure and Transport, were used. First, the curves for grey infrastructure were projected onto the constructed topography through Grasshopper. And to set the height value of the grey infrastructure, the number of floors for the building layer in the digital topographic map was extracted using NGIMap. Then. the hoster reference tool was used so that the number of floors information could be read in Rhino, and a height of 4m per floor was set for multiplication. Through this, the mass of grey infrastructure was built.

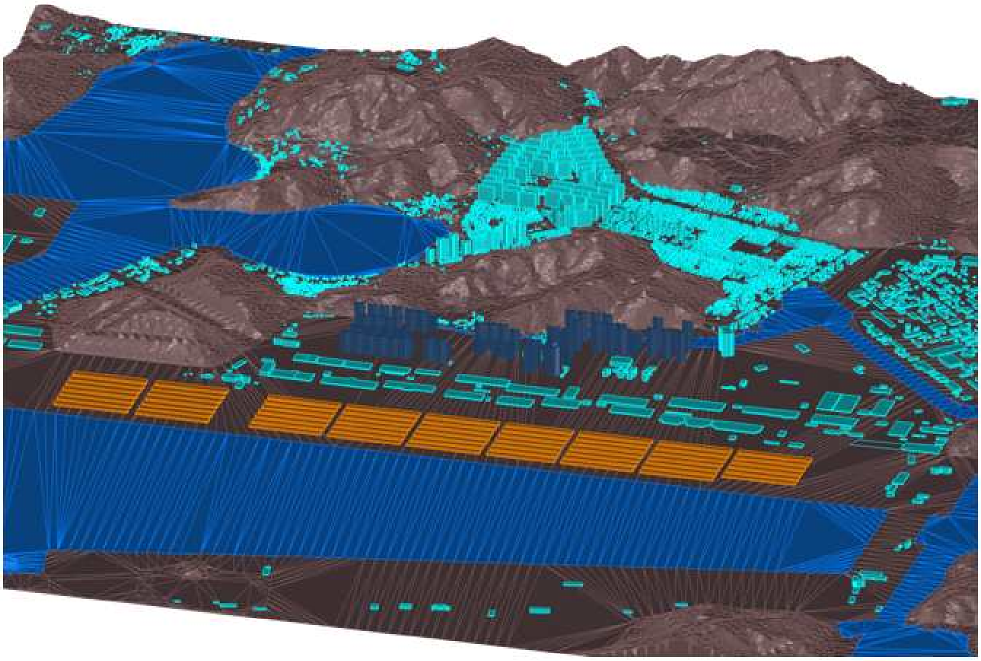

Fig. 7 Model including buildings

3.1.3. Green Infrastructure

In this study, we used both trees and shrubs (hedges) as green infrastructure. We selected green infrastructure based on the form of the horizontal planting in residential areas located in the vicinity of Busan New Port. The form of the trees used in the model had a height of 8 meters and a canopy width of approximately 6 meters, with a trunk diameter of 0.7 times the height. For shrubs, we modeled them in the form of hedges with a height of 1 meter and a width of 0.7 meters. We selected deciduous trees for the horizontal planting consideration. Additionally, since it is difficult to reflect the actual form of trees and shrubs within the model, we modeled the canopy of the trees in a spherical shape and the shrubs (hedges) in a box shape.

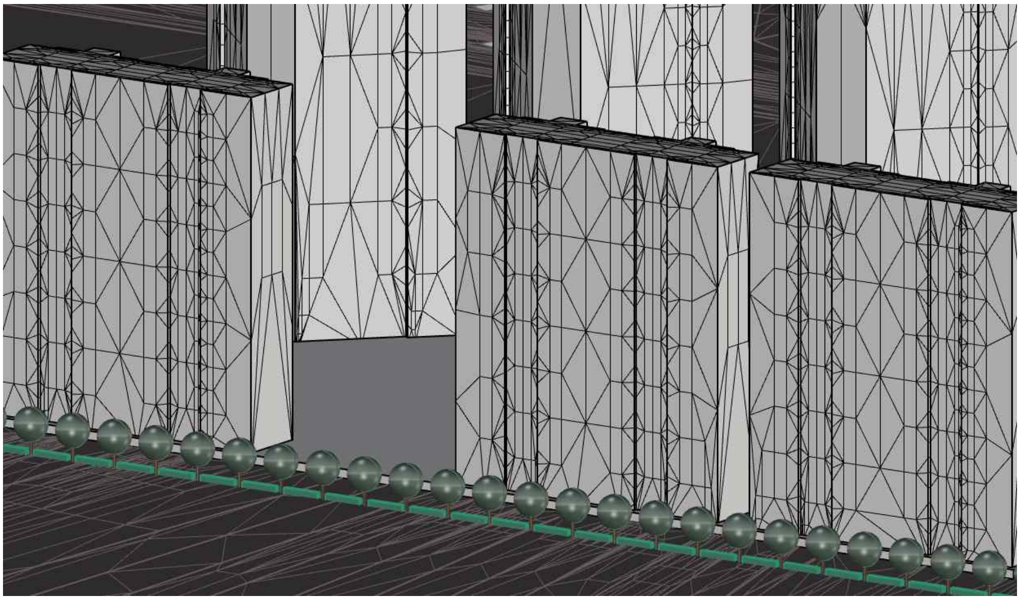

Fig. 8 Green Infrastructure(Tree & Shrub) model

3.2 Calculation of Air Pollutant Emissions

In this study, we aimed to estimate the emissions of particulate matter (PM10) from ships. Referring to the national standards for estimating pollutant emissions from non-road sources and previous studies, we calculated the amount of PM10 emissions from ships. According to the environmental standards provided in Chapter 2, air pollutants emitted from ships are classified into three categories depending on the ship's operation status: anchoring, berthing, and operating mode. However, the CFD model used in this study did not include the areas corresponding to the berthing mode, which is generated when a ship enters the port from the anchoring mode, and the operating mode, which occurs when a ship is sailing on the sea. Therefore, only the PM10 emissions during the anchoring mode were considered.

To estimate the emissions on February 8, 2023, the day with the highest PM10 concentration observed at a monitoring station located inside the ship, we needed the vessel type, gross tonnage (GT), and berthing duration data of ships with arrival and departure records. We collected data on the vessel name and berthing duration of ships that entered or departed during the target period from each dock's website operated in Busan New Port. Additionally, we obtained information on vessel type and GT data from Marine Traffic (www.marinetraffic.com) based on the collected vessel names.

During the application of the collected data to Eq. (5), the national standards focused on macroscopic aspects, providing an average berthing period of 0.79 days. However, we applied the data based on arrival and departure information. Ultimately, the amount of PM10 emitted in the area where ships were berthed was estimated to be 120 μg/m3 on average.

3.3 Computational fluid dynamics

3.3.1 Finite volume method

Computational fluid dynamics is a study that analyzes the physical phenomena of flow by discretizing the governing equations expressing the fluid phenomena to be analyzed as partial differential equations and then calculating them using a computer. In general, the governing equations of fluids are divided into three types(Table. 8): continuity equations, momentum equations, and energy equations. Equations for mass, momentum, and energy, each of which are important physical quantities in a fluid. Nonlinear partial differential equations describing fluid phenomena based on governing equations are Navier-Stokes equations, and additional equation terms are selected according to physical phenomena.

Table. 8 Governing equations of CFD

Equation	Form
Continuity equation	$\frac{\partial \rho}{\partial x}+\frac{\partial(\rho u)}{\partial x}+\frac{\partial(\rho v)}{\partial x}=0$
Momentum equation	$\frac{\partial(\rho u)}{\partial t}+\frac{\partial(\rho u^2+p)}{\partial x}+\frac{\partial(\rho uv)}{\partial y}=\frac{\partial \tau_{xx}}{\partial x}+\frac{\partial \tau_{yx}}{\partial y}$ $\frac{\partial(\rho v)}{\partial t}+\frac{\partial(\rho uv)}{\partial x}+\frac{\partial(\rho v^2+p)}{\partial y}=\frac{\partial \tau_{xy}}{\partial x}+\frac{\partial \tau_{yy}}{\partial y}$
Energy equation	$\frac{\partial(\rho E)}{\partial t}+\frac{\partial(\rho uH)}{\partial x}+\frac{\partial(\rho vH)}{\partial y}=\frac{\partial(u\tau_{xx}+v\tau_{xy}+k\frac{\partial T}{\partial x})}{\partial x}+\frac{\partial(v\tau_{yx}+v\tau_{yy}+k\frac{\partial T}{\partial y})}{\partial y}$

In order to solve the Navier-Stokes equation, which is a partial differential equation, using a computer, the process of converting it into a differential equation, which is an algebraic equation, is essential. In general, methods for differentiating complex partial differential equations into algebraic equations through numerical differentiation include finite difference method, finite volume method, and finite element method. Siemens'

CFD-based simulation software STAR-CCM+ used in this study provides a finite volume method-based solver. This is a method to find out the amount by dividing the calculation area into mesh elements (Computational Cell), storing the material property at the center point of the grid element, and calculating the amount of change in the property value by calculating which flux enters and leaves through the interface of the grid element. It can be said that approximation is made by differentiating the integral governing equation for each mesh element, and approximation is made through a cell-average value and a numerical flux. Since the FVM does not make any assumptions about the shape of the lattice during the differentiation process, it is easy to apply to complex geometry like cities.

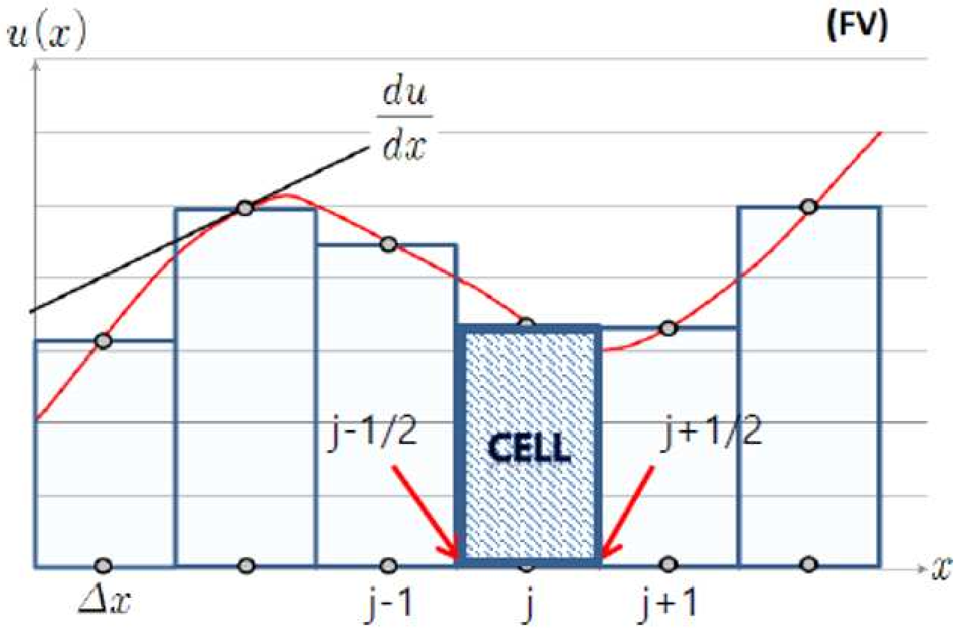

Fig. 9 Concept of FVM

3.3.2 Mesh setting

The simulation process of CFD is divided into three stages. 1) Pre-process stage for modeling the geometry of the analysis area and creating a calculation mesh for the geometry 2) Simulation stage in which a physics model is established based on the governing equations., and boundary conditions and initial conditions are set to proceed with the analysis 3) Post-process stage to visualize calculation results and analyze numerical solutions. The grid generation step included in the pre-process stage is a process of discretizing the spatial domain into very small mesh elements so that fluid particles assumed to be continuum can be calculated by computer. There are three core grid cells that can be created in STAR-CCM+. A tetrahedral cell useful for finite element (FE) solvers, polyhedral cell that is numerically more stable by merging tetrahedral cells and is suitable for heat transfer analysis between fluids and solids, trimmed hexahedral cell that is generated by aligning it with the Cartesian axis and is effective for external aerodynamic analysis(Fig. 10).

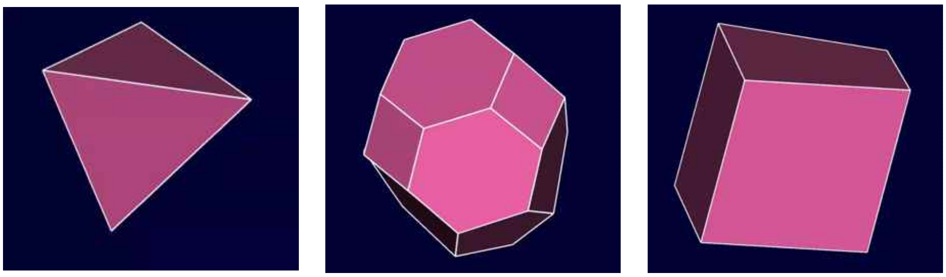

Fig. 10 Types of mesh in CFD

In this study, trimmed hexadral was used for the analysis of fine dust according to the flow of the external atmosphere. The mesher used to set the grid is as follows:

- Surface Remesher
- Automatic Surface Repair
- Trimmed cell mesher
- Prism layer mesher

When setting the mesh in the flow analysis of fine dust, it is necessary to set the mesh more densely for obstacles such as buildings or external domains. In addition to the basic default control, additional surface control was applied to buildings, containers, and apartments that serve as structures in this study. In addition, additional surface control was applied to the side and sky that serve as outwall in the analysis domain. In case of green infrastructure, it requires more detailed interpretation due to its small size compared to other geometries. Therefore, we set a denser cell condition in order to capture the details more accurately. Table. 9 represents mesh setting value of all geometries in the domain model.

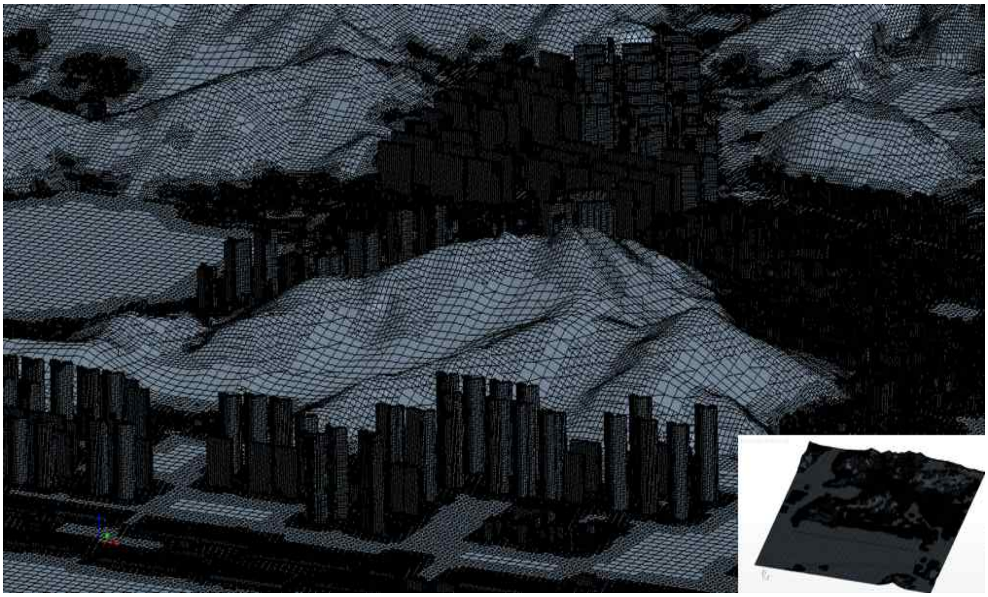

Fig. 11 Result of mesh operation

Table. 9 Mesh setting value

Default control	Values	
Base size	20.0m	
Prism layer total thickness	20.0 (Relative to base)	
Volume growth rate	Default growth rate	Medium
	Surface growth rate	Medium
Maximum cell size	1000.0 (Relative to base)	
Custom control (Structure)	Values	
Target surface size	10.0 (Relative to base)	
Prism layer total thickness	2.0 (Relative to base)	
Minimym surface size	1.0 (Relative to base)	
Custom control (Outwall)	Values	
Target surface size	1000.0 (Relative to base)	
Minimum surface size	50.0 (Relative to base)	
Custom control (Green Infrastructure)	Values	
Target surface size	1.0 (Relative to base)	
Minimum surface size	0.5 (Relative to base)	

3.3.3 Physics setting

Diffusion analysis of pollutants such as fine dust in CFD can be analyzed in two ways: the Lagrangian model and the Eulerian model. The Lagrangian model is a method of performing flow analysis for each particle moving in the flow field within the domain. This is a method of calculating the movement of particles by scattering particles on them using the results of wind environment analysis. The Eulerian model is a method of analyzing flow rather than calculating changes in particle behavior in a flow field. The flow of air in the flow field is calculated through momentum and turbulence equations, and only the fine dust concentration is calculated separately based on this. In this study, the Eulerian model was used because it aims to improve the concentration of fine dust in residential complexes through simulation. Fine dust diffusion analysis using the Eulerian model calculates the diffusion of air and fine dust using a multi-component physical model. Compared with the physical model used in the wind environment, which is the basis of the analysis of fine dust, a non-reacting model was used to assume that each gas component does not react with each other using the multi-component gas model, and the energy equation was calculated. Segregated fluid temperature model was used. The physics models of wind environment analysis and Eulerian analysis are summarized at Table. 10.

Since the basic physical properties of fine dust are not provided in STAR-CCM+, the physical properties of fine dust must be separately entered in the multi-component gas model. The fluid properties that can be entered in the multi-component gas model are density, dynamic viscosity, molecular weight, and specific heat (Table. 11).

The initial condition in this analysis was assumed to be 100% full of clean air. To simulate this in the model, the species mass fraction was designated as [1, 0]. Mass fraction is the mass ratio of air, and the sum of the twoselected in the multi-component gas model is 1.

Table. 10 Comparison of model used in wind environment & Eulerian model

Wind environment	Eulerian model
• Three dimensional • Gradients • Steady • Gas • Segregated flow • Constant density • Turbulent • RANS Realizable K-epsilon turbulence • Exact wall distance • Two-Layer all y+ wall treatment	• Three dimensional • Gradients • Steady • Segregated flow • Constant density • Turbulent • RANS Realizable K-epsilon turbulence • Exact wall distance • Two-Layer all y+ wall treatment • Multi-component gas • Non-reacting • Segregated fluid temperature

Table. 11 Properties of fine dust

Property	Value
Density	1640.0kg/m³
Dynamic viscosity	1.91925E-5 Pa-s
Molecular weight	30.0kg/kmol
Specific heat	999.431J/kg-K

3.3.4 Boundary condition

3.3.4.1 Fine dust

To set the boundary condition for where the fine dust will be generated, the field function within the program was used to specify the boundary range and the amount of generation. For the location of the generation, the part of the model where the ship is docked was separated and set to generate 120 μg/m3 of PM10, as calculated in section 3.2. To simulate the scenario where the PM10 moves from the harbor to residential areas, values for wind direction and speed were inputted into the side wall of the domain. The wind speed was set to 2 m/s and the wind direction was set to the north, as it was predicted that PM10 would be distributed most heavily in the residential area. Wind direction to the north is main direction of site at summer (Han, 2020).

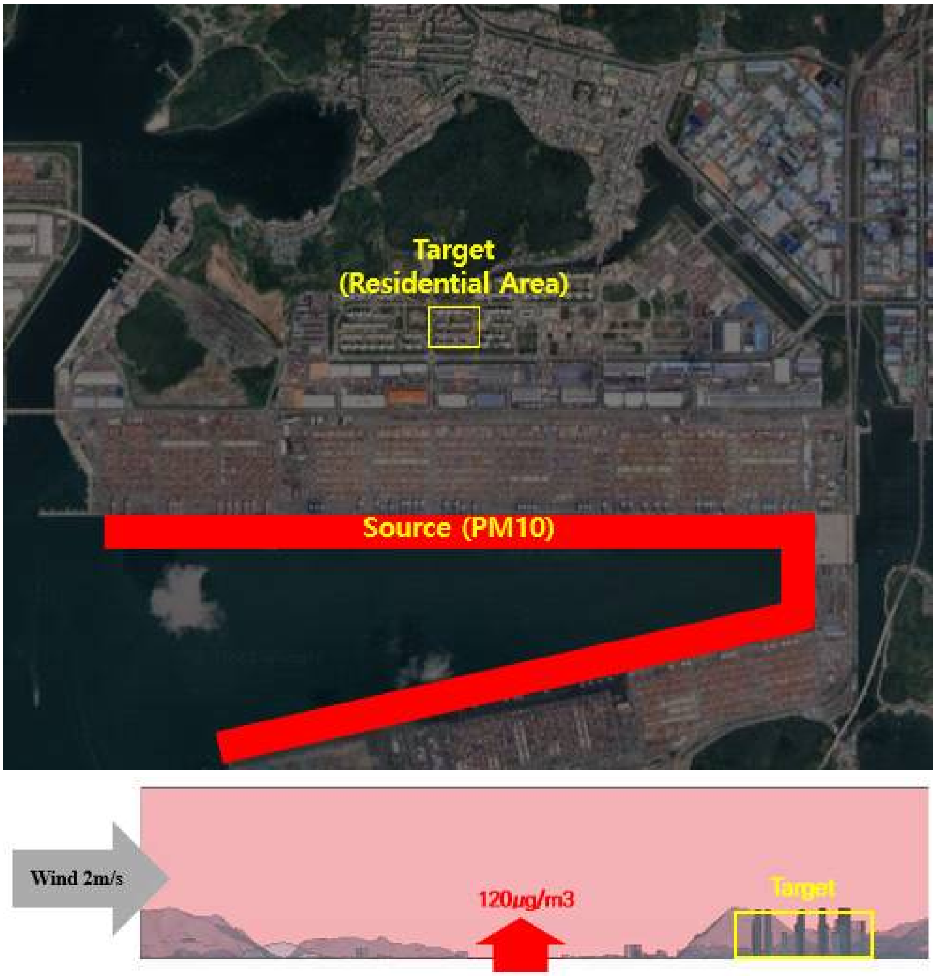

Fig. 12 Schematic diagram of Boundary condition

To simulate the situation where 120 ㎍/m3 of PM10 is generated at the location, the mass fraction of PM10 was calculated and inputted. The mass fraction of PM10 was calculated by dividing the density of PM10 by the density of air, and the sum of the mass fraction of air and PM10 is equal to 1. When approximately 120 μg/m3 of PM10 is generated, the mass fraction of air and PM10 is [0.999999898661, 1.01339 e-07], and this was set as the boundary condition for the source. Furthermore, clean air was assumed for the wind, and the mass fraction of air and PM10 was set to [1, 0].

Table. 12 Summary of boundary condition

Parameter	Value
Side	
Boundary type	Velocity Inlet
Velocity specification	Components
Velocity	[0.0, 2.0, 0.0] m/s
Species mass fraction	[1, 0]
Source	
Boundary type	Velocity Inlet
Species mass fraction	[0.999999898661, 1.01339 e-07]

3.3.4.2 Green Infrastructure

As mentioned in the literature review, previous studies on using CFD for improving air quality through green infrastructure have shown that three effects (aerodynamic effect, deposition effect, resuspension effect) can be simulated. This study aims to apply the first two effects, as the resuspension effect has not been widely studied and has limited references.

For the aerodynamic effect, Eq. (2) and (3) mentioned earlier were used. As STAR-CCM+ does not provide these equations, they were applied using field functions. The values of variables in the equations were determined based on previous studies. The drag coefficient C_d was set to 0.2 in the CFD model to reflect the average value instead of a specific value for each species (Gromke & Blocken, 2015a). For tree species, the leaf area density (LAD) value for the summer season, when leaves are abundant, was applied.

Jeanjean et al. (2017) used a LAD value of 1.6 for deciduous trees in the summer. For shrubs, LAD values range from 2 to 5 (Vos et al. 2013), and the average value of 3.5 was applied in this study. The values of β_p and β_d were set to β_p=1 and β_d=4, based on previous studies (Lie et al. 1996, Katul et al. 2004, Amorim et al. 2013, Salim et al. 2015). The model constant $C_{\epsilon 4}$ and $C_{\epsilon 5}$ were set to the values of $C_{\epsilon 4}$=1.5 and $C_{\epsilon 5}$=1.5, which were used in modeling urban vegetation (Amorim et al. 2013, Hong et al. 2018).

The deposition effect, which simulates the phenomenon of fine dust being absorbed by the green part of green infrastructure, was applied using Eq. (4) as mentioned earlier. For LAD, the values applied in Eq. (2) and (3) were applied. The deposition velocity V_d of PM10 was referenced from previous studies. The values for V_d of PM10 varied in previous studies. Vos et al. (2013) stated that it ranges from 0.2 to 1, while Vranckx et al. (2015) applied V_d value ranging from 0.5 to 5. In this study, a value of V_d 2m/s was applied for PM10.

3.3.5 Simulation scenarios

The purpose of this study is to derive the quantitative effect and what type of green infrastructure arrangement has the optimal effect when green infrastructure is applied to the residential complex behind Busan New Port. One of the residential complexes was selected, and various scenarios for street planting were set around the residential complex.

In order to diversify the planting type, various changes were made vertically and horizontally. Vertically, shrubs were added to the trees mainly used in previous studies. Horizontally, according to the presence or absence of trees and shrubs, it was divided into three categories: the case with only shrubs, the case with only trees, and the case with both, and the planting arrangement was divided into rows 1 and 2.

In addition, the spacing of trees was additionally divided into five at 2m intervals from 6m to 14m. A total of 30 scenarios were classified. Additionally, as the distance between trees increased, the amount of shrubs was increased. The location and of target residential complex is showed in fig. . Fig. 14-19 are perspective for each scenario

To derive the optimal scenario based on the type of vegetation in green infrastructure, criteria were established. In this study, the scenario with the lowest average concentration in a 1.5 m cross-section within a residential complex, taking into account the height of pedestrians, was defined as the optimal scenario.

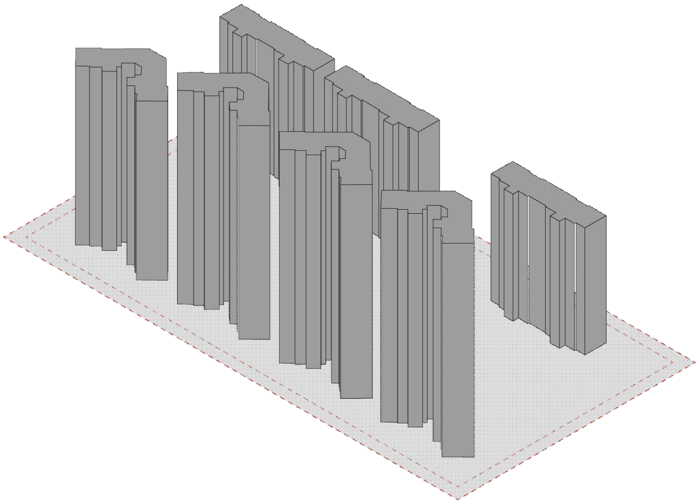

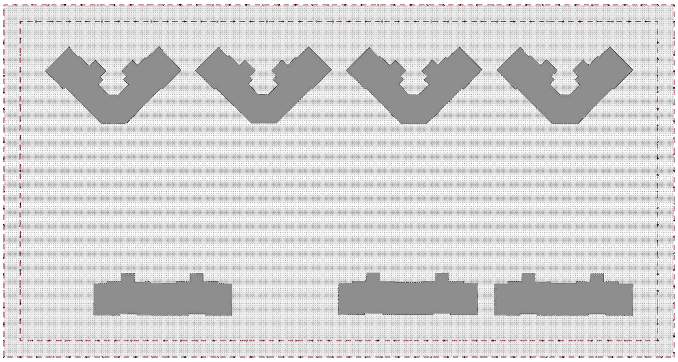

Fig. 13 Plane and perspective of target

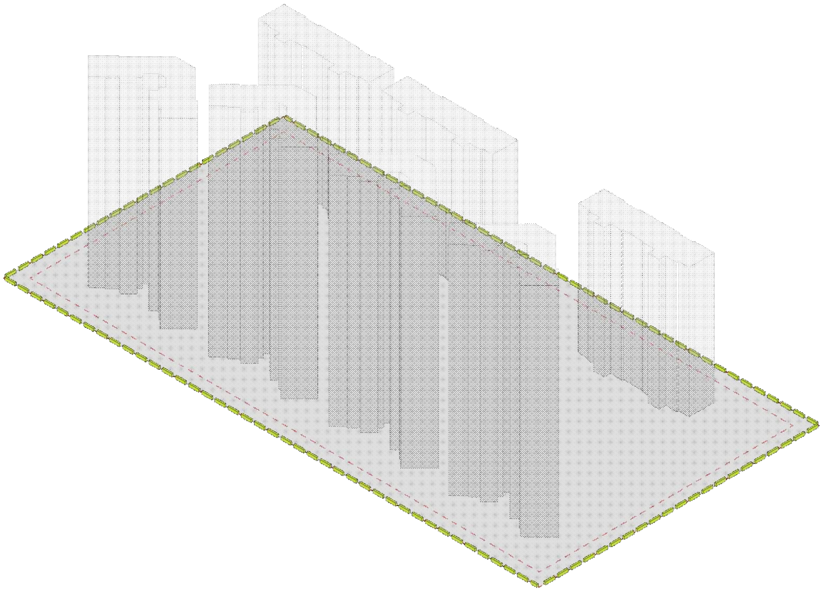

Fig. 14 perspective of shrubs row1 scenario

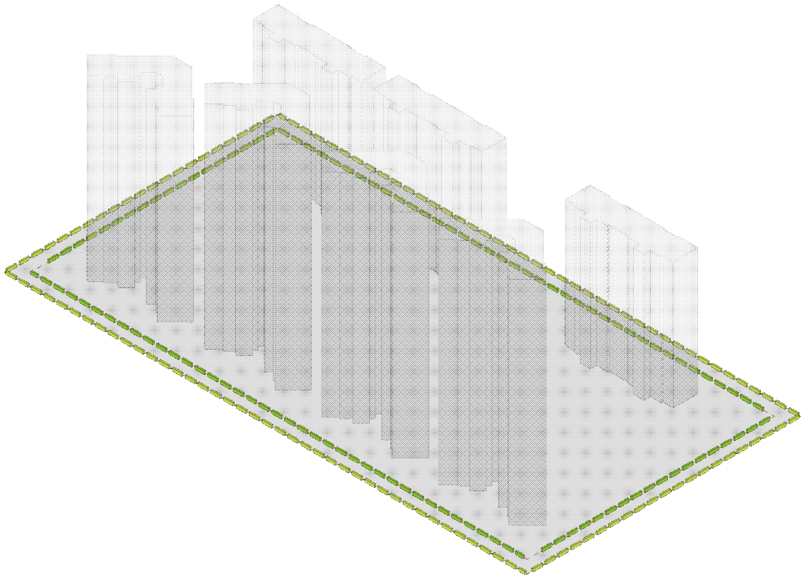

Fig. 15 perspective of shrubs row2 scenario

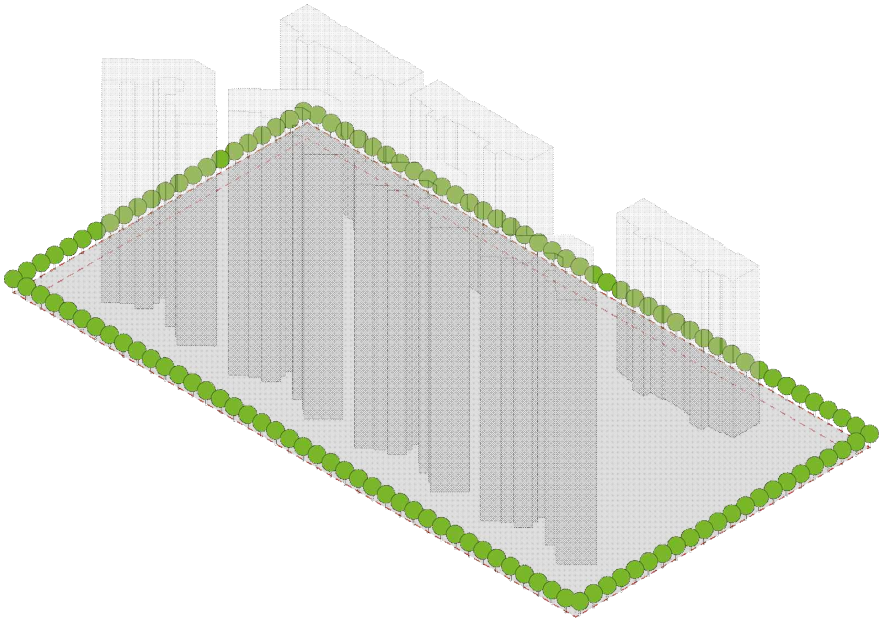

Fig. 16 perspective of trees row1 scenario

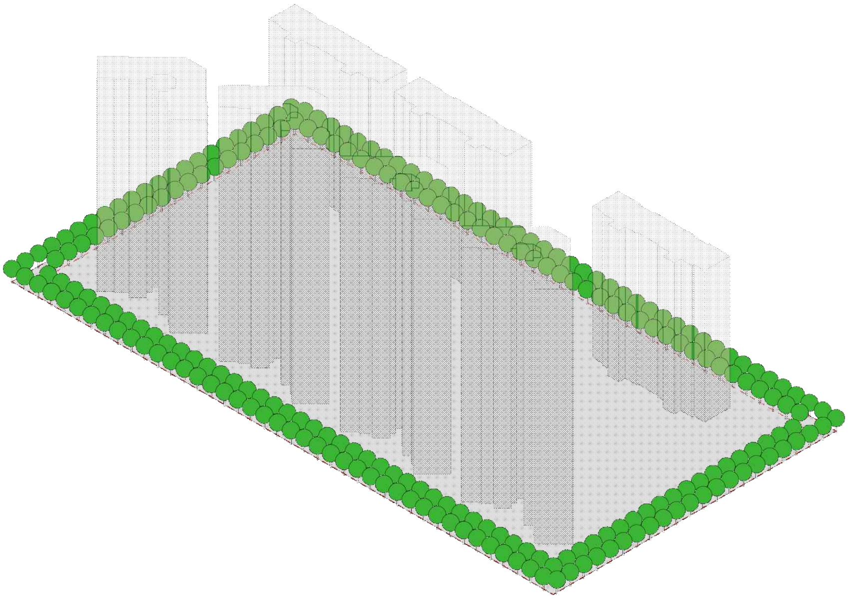

Fig. 17 perspective of trees row2 scenario

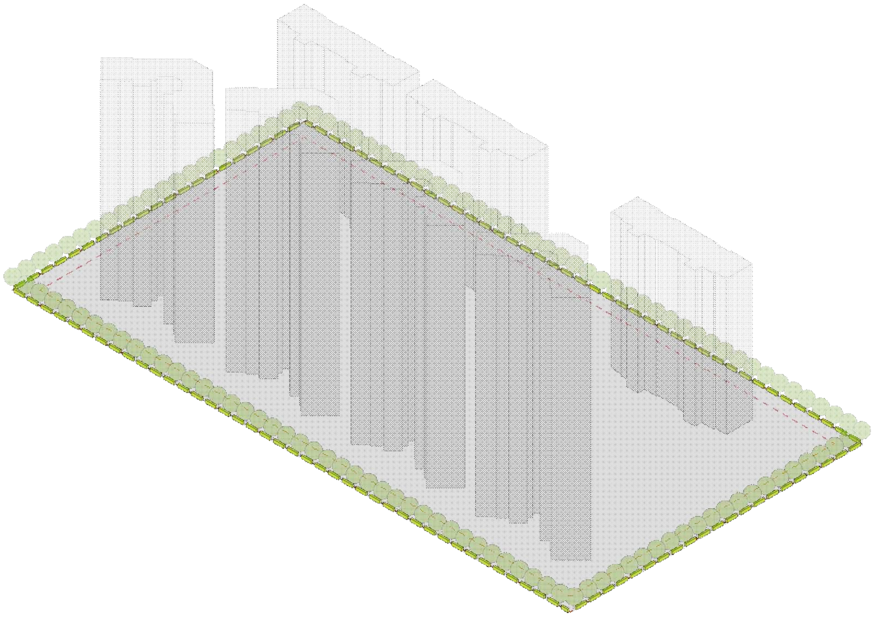

Fig. 18 perspective of shrubs and trees row1 scenario

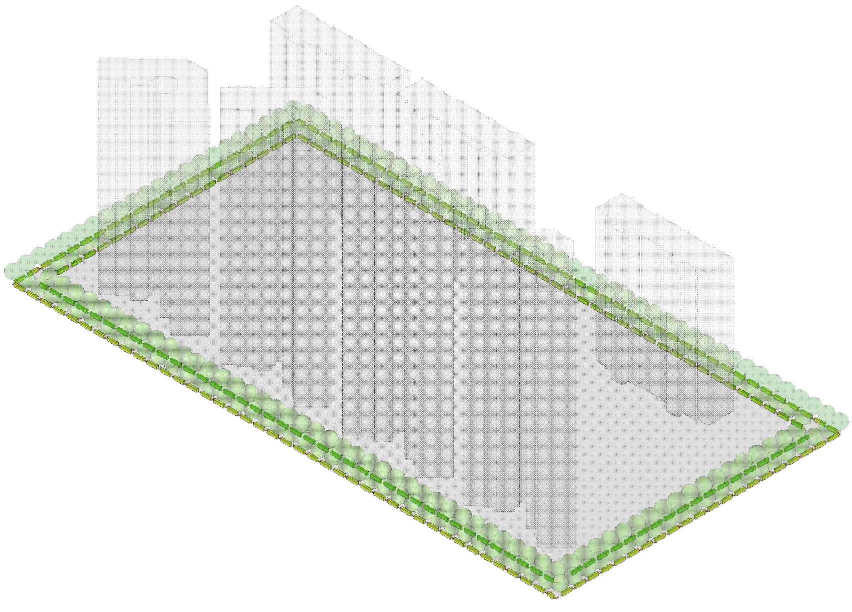

Fig. 19 perspective of shrubs and trees row2 scenario

3.4 Model verification

For verification of a CFD model, the model was simulated using data from February 8, 2023, for the amount of fine dust emissions caused by a ship. The emission data, as well as the wind direction and speed information, were applied to the CFD model for comparison with the data obtained from two fine dust observation stations located within the model area.

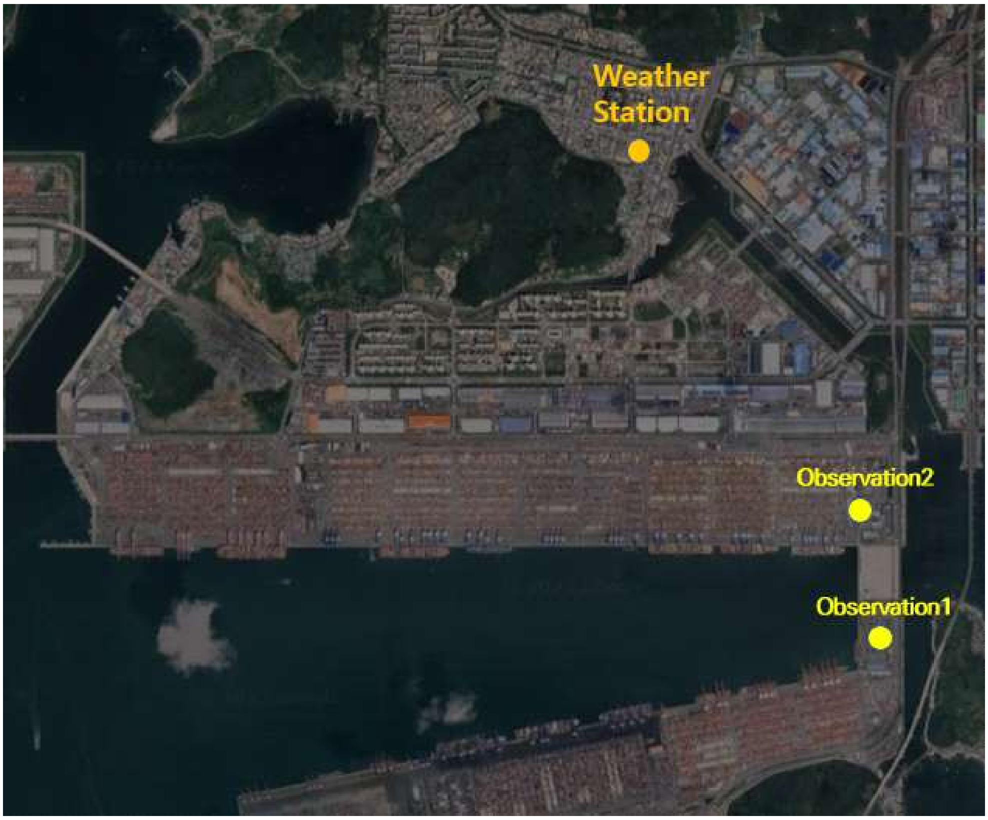

Fig. 20 Location of weather station and PM10 observation station

The emissions data was determined to be 120 µg/m3 which was calculated at chapter 3.2, and the wind direction and speed were obtained from the weather station within the model. The distance between the weather station and the fine dust observation stations is approximately 2 km, which was seemed suitable for this study. Both fine dust observation stations are located within Busan New Port.

The PM10 data provided by the observation stations were provided at hourly intervals. For this study, only the data with a PM10 concentration of 80 µg/m3 or higher were used for the time period from 1:00 a.m. to 11:00 a.m. for a total of 11 data points, which were compared with the simulation values. Fig. 20 shows the location of the weather station and the fine dust observation stations within the CFD model.

Chapter 4. Results

4.1 Model verification

To validate a CFD model, PM10 data from two observation stations Obs 1, Obs 2 and data from two locations where the observation sites are located in the simulation were analyzed. Fig. 21, 22 show the Obs 1, Obs 2, and simulation values. Table. 13 is summary of the wind direction and speed data used in the simulation, as well as the PM10 concentrations in the observation and simulation.

Table. 13 Summary of value for model verification

Time	Wind Direction (deg)	Wind Velocity (m/s)	Simulation 1 (μg/m3)	Obs 1 (μg/m3)	Simulation 2 (μg/m3)	Obs 2 (μg/m3)
01:00	225.2	0.1	59.47	71	75.14	85
02:00	286.2	0.5	106.74	90	78.93	85
03:00	231.5	0.3	79.40	79	70.41	75
04:00	351.2	0.4	80.94	76	60.29	70
05:00	282.7	0.1	112.10	92	75.55	92
06:00	291.8	0.4	104.21	90	86.07	86
07:00	255.2	0.1	82.84	84	93.18	98
08:00	193.4	0.2	100.79	91	78.29	100
09:00	288.3	0.6	117.47	93	103.41	109
10:00	248.8	0.9	111.43	107	93.88	97
11:00	332.1	2.4	117.52	99	76.80	88

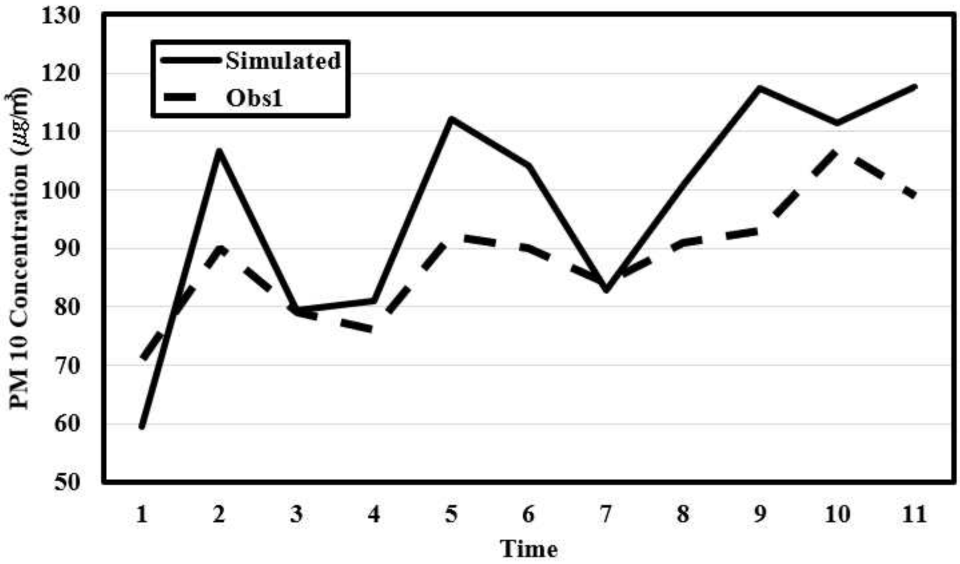

Fig. 21 Observation and simulated value of Obs 1

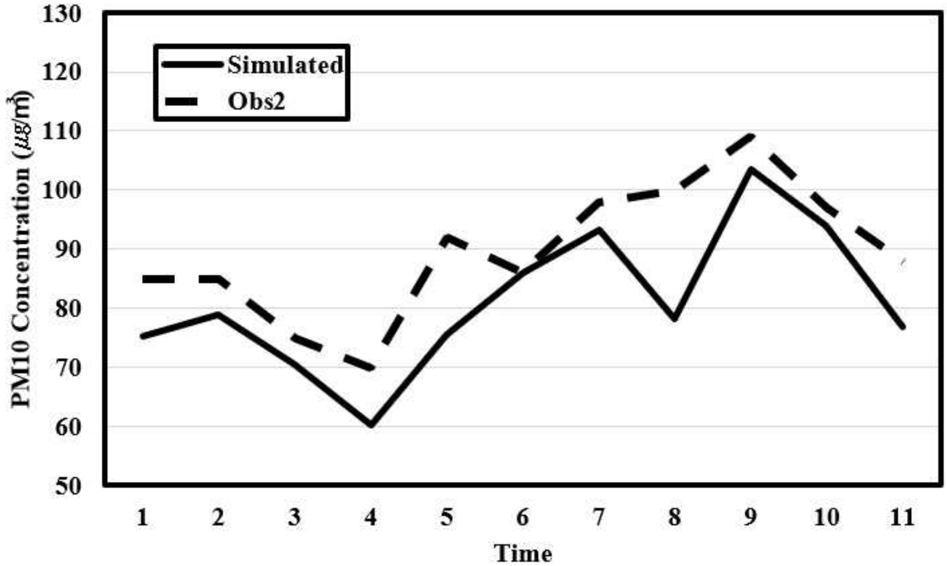

Fig. 22 Observation and simulated value of Obs 2

When comparing the observation and simulation value for Obs 1, the range of value was 71-103µg/m3 for the observation and 59-117µg/m3 for the simulation, with mean values of 88.4µg/m3 and 97.5µg/m3, respectively. The simulation values tended to be higher overall. For Obs 2, the range of values was 70-109µg/m3 for the observation and 60.3-93.9µg/m3 for the simulation, with mean values of 89.5µg/m3 and 81.1µg/m3, respectively. In contrast to Obs 1, the simulation values tended to be lower. When comparing the observation and simulation values, both data sets showed some deviation. This was attributed to the limitations in data collection for PM10 emissions from other sources like transport facilities other than ships and the inability to use accurate wind direction and velocity data at the verification location.

However, when performing correlation analysis for the observation and simulation values at the two locations, both points showed a coefficient of determination of 0.7 or higher. This suggests that the CFD model used in this study has a reasonable correlation with reality.

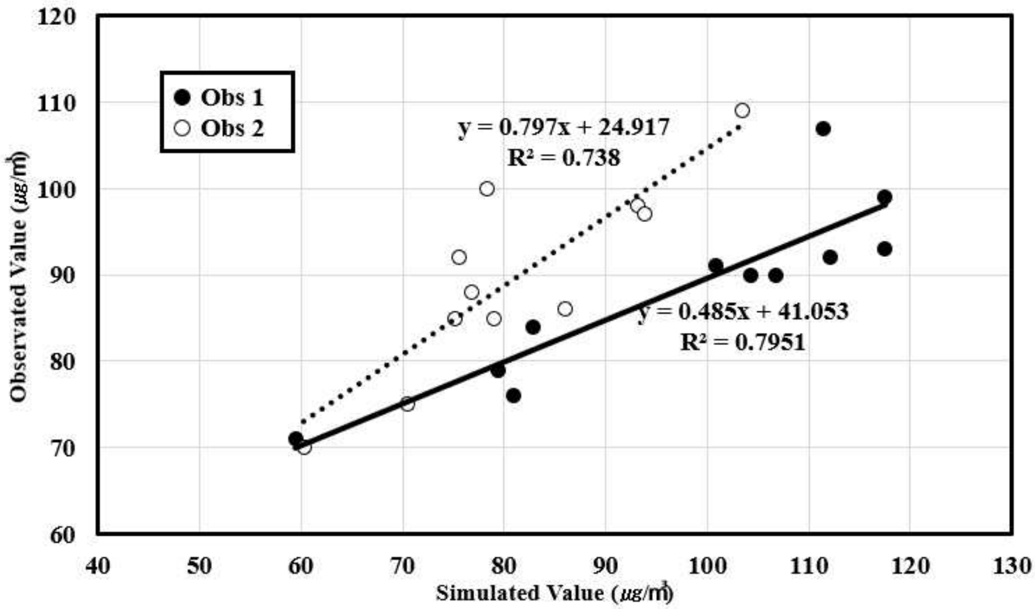

Fig. 23 Correlation analysis results of observation and simulated value

4.2 Green Infrastructure Scenario

A scenario analysis was conducted based on a verified model, and CFD simulation was performed for a Base case that does not have a Green Infrastructure that can be used as a comparison group with various Green Infrastructure scenarios. The fine dust emission level was set to 120µg/m3, the same as in the verification, and the wind direction was set to south, which is the high fine dust period within the target area during the summer season. The average concentration of the section at a height of 1.5m from the ground, which is the height of a person, was chosen as the value to be compared for each case, the value for the Base case was 68.04µg/m3[Fig. 24].

The results of the simulation are summarized in [Table. 14], where trees are represented as T and shrubs (hedges) are represented as H and in the case of TH, trees and shrubs are present together. The PM10 reduction effect for each green infrastructure scenario varied from a minimum of 0% to a maximum of 30%, except for cases where the concentration was higher than the base.

In the case of only trees (T_row1, T_row2), a similar pattern was shown according to the interval when comparing scenarios with row 1 and 2. The reduction effect was found to be the lowest in both rows 1 and 2 of the 6m case where the planting interval was narrow and the amount of planting was the highest. In addition, the highest reduction effect was shown at 8 m thereafter, and the effect decreased as the interval became wider. Contrary to the general idea that a large amount of trees would be more effective in reducing PM10, in this study, the effect was not good even if the amount of trees was large, and also the planting interval was too wide.

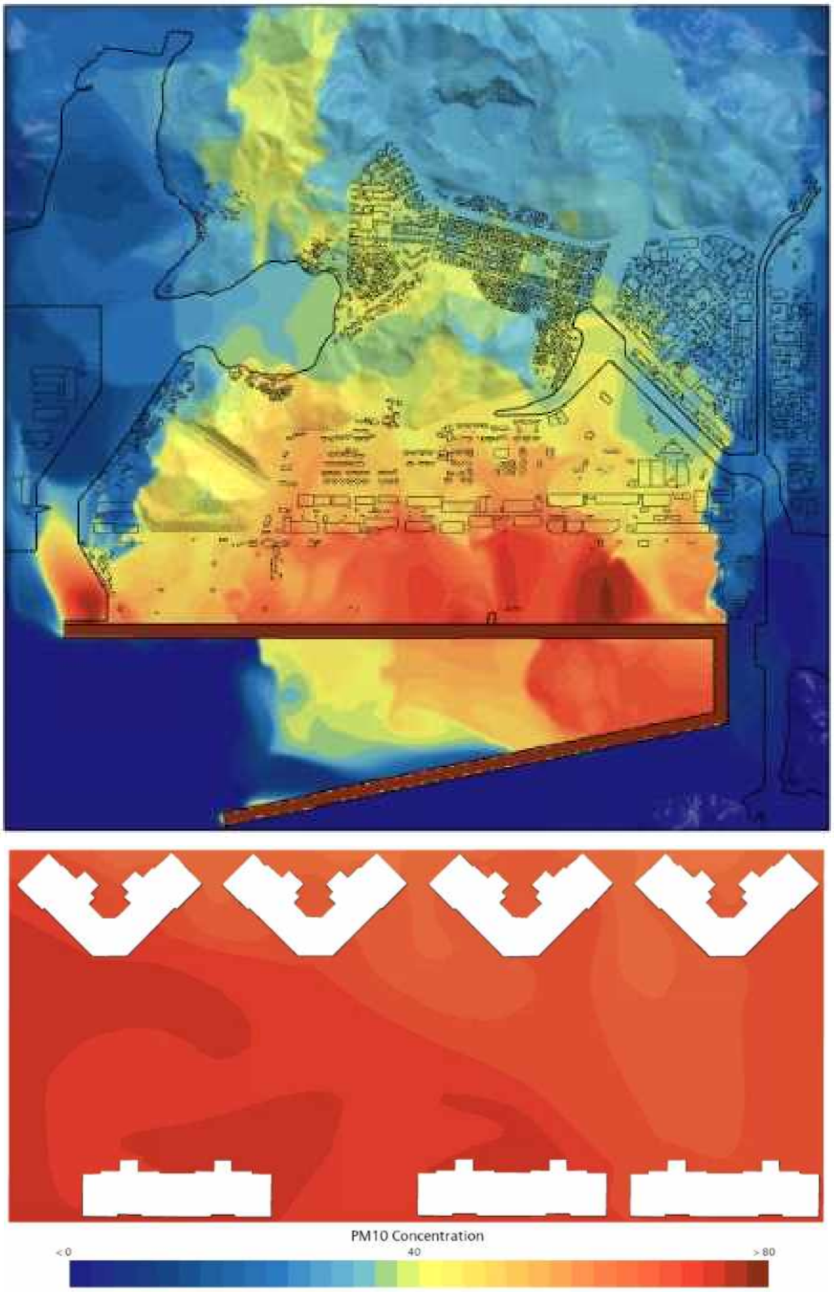

Fig. 24 Simulation results of Base case

Table. 14 Simulation results of green infrastructure scenarios

Interval	6m 1.5m Section	Value	8m 1.5m Section	Value	10m 1.5m Section	Value	12m 1.5m Section	Value	14m 1.5m Section	Value
T_row1	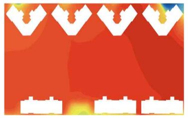	64.04 (-5.88%)		57.02 (-16.20%)		60.56 (-10.99%)		61.24 (-9.99%)		63.27 (-7.01%)
T_row2	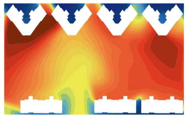	58.76 (-13.64%)	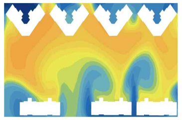	49.34 (-27.48%)		52.98 (-22.13%)	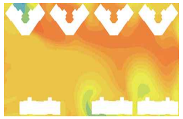	54.35 (-20.12%)		56.95 (-16.30%)
H_row1	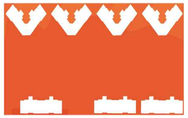	68.19 (+0.22%)		65.43 (-3.84%)		65.91 (-3.13%)		72.49 (+6.54%)		66.36 (-2.47%)
H_row2	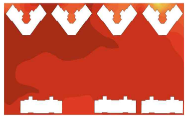	70.84 (+4.12%)		63.25 (-7.04%)		66.86 (-1.73%)	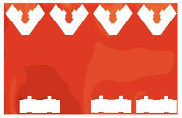	67.37 (-0.98%)		65.27 (-4.07%)
TH_row1	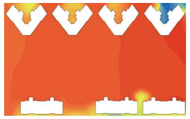	64.56 (-5.11%)		58.78 (-13.61%)		62.14 (-8.67%)		61.46 (-9.67%)		60.31 (-11.36%)
TH_row2		59.31 (-12.83%)	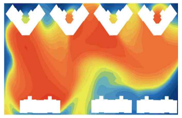	47.21 (-30.61%)		52.61 (-22.68%)		53.87 (-20.83%)	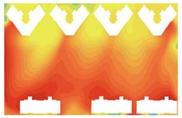	54.69 (-19.62%)

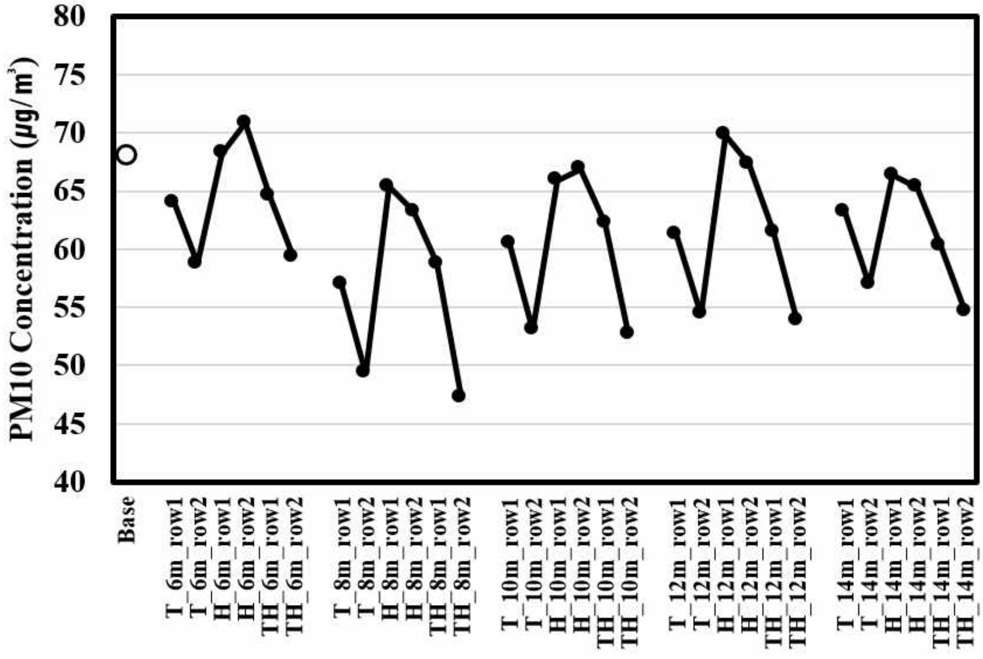

Fig. 25 Simulation results of green infrastructure scenarios (interval)

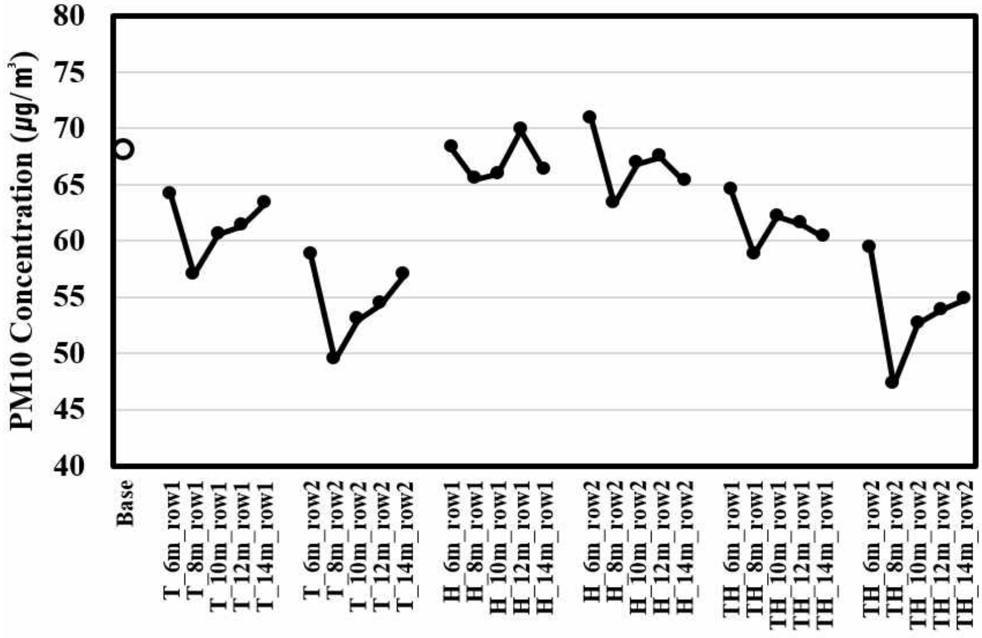

In the case of shrubs (H_row1, H_row2), the reduction effect was the highest at 8m, the same as the case of trees. However, unlike trees, it was found that there was no specific pattern when compared by interval.

When comparing trees and shrubs, the reduction effect was about 5% to 16% in case of T_row1 and 13% to 27% in T_row2. In case of the H_row1, the maximum was 3.8% and in H_row2, the maximum was 7%. Also, in case of shrubs, the PM10 concentration was higher in some cases than in the base case without green infrastructure. It was found that the PM10 reduction effect of trees overwhelming that of shrubs.

Comparing TH with trees that had a high PM10 reduction effect, it was confirmed that TH showed a similar pattern to the analysis results of trees. Comparing T_row1 and TH_row1, the case with only trees appeared to be more effective, and in the case of row2, the effect of TH was found to be better. However, the difference between the two planting types was about 3% at most, indicating that the effect obtained by additionally planting shrubs was very small. In addition, when comparing the PM10 concentration contour of the target area, the internal concentration was higher in TH_row2, which had a better effect than that of tree trees. Additional planting of shrubs can improve the mitigation effect in the periphery, but it is presumed that excessive planting rather inhibits atmospheric circulation and increases the concentration in the inner area.

4.3 Aerodynamic vs. Deposition

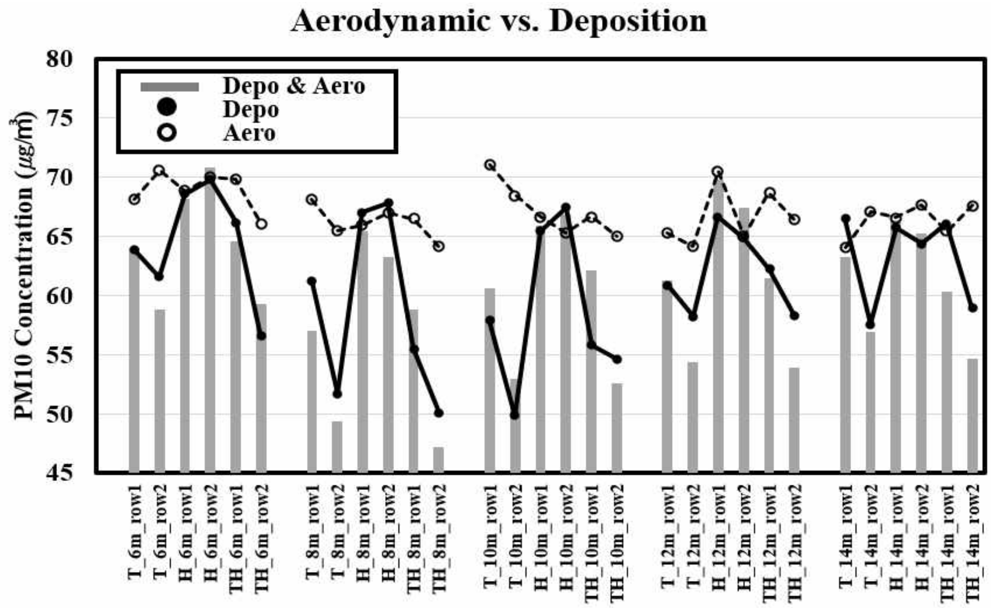

Fig. 27 Simulation results of aerodynamic & deposition effect

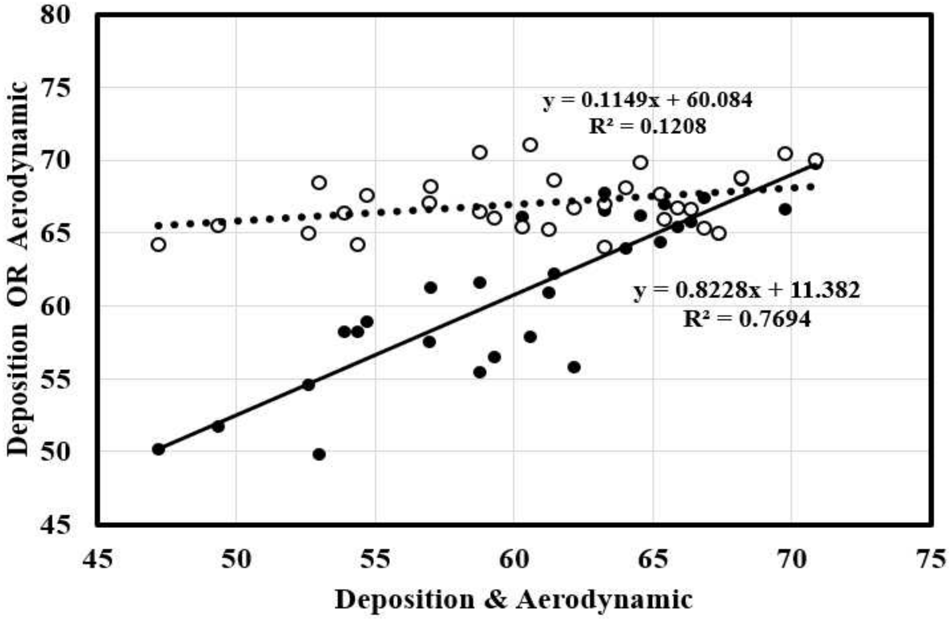

In the study, 30 scenarios were analyzed incorporating both aerodynamic effects and deposition effects simultaneously. The aim was to identify to what extent the two mechanisms for reducing particulate matter, applied in this study, correlate with the total outcomes derived from previous analyses. Analyses were executed for 60 cases, distinguishing scenarios with only aerodynamic effects from those with only deposition effects among the 30 scenarios. The findings indicated a similar pattern with the initial results for the case of the deposition effects. However, no specific pattern was observed in the case of aerodynamic effects. Upon conducting a correlation analysis with the original results, the R^2 value was approximately 0.77 for the deposition effects, and 0.12 for the aerodynamic effects. While the adsorption effects showed a reasonable correlation with the initial results, the aerodynamic effects were found to have a significantly low correlation.

Chapter 5. Discussion

5.1 Simulation model

The most challenging aspect of simulating urban environmental issues such as heatwaves, not just PM10 (air quality), is how accurately the terrain and infrastructure of urban areas are represented and how closely the simulation aligns with reality. In this study, to construct a more accurate model, a numerical terrain model including the terrain and surrounding infrastructure was created using 3D CAD Rhino and Grasshopper. In contrast to previous studies that simplified and generalized a portion or a specific form of the city to build the model, this research constructed the terrain and infrastructure for a 6km x 6km area.

For model validation, the estimated amount of PM10 expected to be generated in the area where ships are docked was calculated based on formulas, and data from two PM10 monitoring stations located within the model domain, which can be compared with the estimated values, were utilized. Additionally, environmental data (wind direction, wind speed) used as inputs for the model domain were obtained from weather observation stations. When compared to the points within the domain that corresponded to the locations of the PM10 monitoring stations, the correlation showed a compliance with an $R^2 \geq 0.7$. Although the overall trends were similar, there was a bias between the observed values and the simulation values. While the model constructed in this study can be considered reasonably accurate due to the similarity in trends, the presence of slight bias indicates a lack of precision in the model. This could be attributed to the selection of the closest point for weather data, which may have introduced errors due to localized differences in weather conditions. Additionally, the model did not consider emissions from factors such as construction machinery and other sources in the port area, apart from emissions from ships. Considering real measurement data and the surrounding environment at the desired locations during the model validation process would lead to better research outcomes in the future.

5.2 GI scenario

One of the major differentiating factors of this study compared to previous research is the detailed scenario analysis of Green Infrastructure (GI). Previous studies did not differentiate tree spacing in their analysis scenarios and only considered a single type of vegetation. However, in urban areas, the types of vegetation in GI can vary, and the spacing of vegetation is determined by regional policy standards. In this study, we considered the inclusion of trees and shrubs in roadside plantings for PM10 reduction and divided the spacing into a range from 6m to 14m. We investigated how the PM10 reduction effect varies according to the spacing, and the scenario with the maximum effect was found to have a spacing of 8m. Interestingly, the height of the trees in this scenario was 8m. While this may be a coincidence, it can be speculated that the relationship between tree height and spacing may also influence the reduction of PM10. If future studies further refine the spacing and also consider the height of the vegetation, this study can further advance and produce meaningful results.

Another significant finding is the prioritization of performance considerations when applying green infrastructure for PM10 reduction. The results of this study ultimately indicate that surface characteristics and absorption performance, such as porous structures, are more dominant in changing the surrounding airflow dynamics than the aerodynamic effects. Depending on the type of vegetation, GI can have superior absorption capabilities for PM10 or may exhibit better resistance to wind. The PM10 reduction effect can vary depending on the tree species applied. This information can serve as a reference for future related studies.

Regarding the parameters used to simulate the PM10 reduction performance of GI in this research, previous research values were referenced due to limitations in the research conditions. Previous studies tended to present GI parameters based on seasonal variations (leafy in summer, leafless in winter) or specific tree species. However, to apply more accurate parameters, it is necessary to devise parameters that can be incorporated into CFD models based on performance experiments conducted on individual GI components. Furthermore, since the results are only within the CFD model, cross-validation with real-field results will further enhance the quality of the research.

Chapter 6. Conclusion

The objective of this study was to analyze the effects and derive efficient design methods when introducing green infrastructure in residential areas behind port regions, which are at risk of air quality deterioration due to large amounts of particulate matter emitted from ships. This study quantitatively analyzed the PM10 reduction effect of trees and shrubs (living fences) in Busan New Port, the largest port in South Korea, in the city of Busan. To apply an efficient green infrastructure, scenarios were finely divided according to planting type and spacing, and a CFD model capable of fluid analysis in large spaces was used to evaluate the effects. The validation of the CFD model was performed using ship entry and exit information, and wind direction and speed data that affect the dispersion of particulate matter. Subsequently, comparative analysis was conducted for 30 green infrastructure scenarios and a Base with no green infrastructure through steady analysis in the CFD model. Through the results of this study, four conclusions can be derived.

Green infrastructure is generally known to be an essential element for the sustainability of humans and the environment, and it is recognized that the more of it, the better. However, this study yielded results contradicting this common belief. When comparing by spacing, the scenario with the most planting quantity, 6m, showed the least reduction effect, while 8m demonstrated the best, and the effect decreased as the spacing increased. When introducing green infrastructure to improve air quality, it is deemed necessary to set an appropriate spacing aligned with the budget and scale of the project for optimum effects.

The PM10 reduction effect appeared to be higher in trees than in shrubs. The average reduction rates of scenarios with only trees or shrubs (T_row1, T_row2, H_row1, H_row2) were 10.01%, 19.93%, 0.53%, and 1.94%, respectively. For mixed scenarios (TH_row1, TH_row2), the difference with tree-only scenarios was negligible. Thus, when introducing green infrastructure to improve air quality, it is inferred that incorporating trees would be more effective.

This study applied the aerodynamic effect and the deposition effect as the PM10 reduction mechanisms of green infrastructure. The results considering both effects simultaneously were compared with those considering each effect separately. The outcome incorporating both effects and the deposition effect showed a correlation of $R^2 = 0.77$, while the aerodynamic effect indicated a correlation of $R^2 = 0.12$. The aerodynamic effect is thought to have large fluctuations as the form of the scenario changes. Decision-makers, when establishing a planting plan for air quality improvement, should prioritize considering the deposition performance of green infrastructure and make decisions suitable for the site.

However, there are two limitations in this study. First is the accuracy of the model. To derive more precise results, various factors influencing particulate matter should be considered. A modeling method that reflects existing green infrastructure and climatic conditions such as temperature and humidity should be constructed. The second is the singularity of the green infrastructure form. The reduction performance will vary depending on the shape and size of the green infrastructure, and the results will vary accordingly. It is important to compile data and design according to factors such as size and leaf area density for various species. If these two limitations are addressed, this study can evolve into a more substantial research.

초 록

- 항만지역 배후 주거단지 대기질 개선을 위한 효율적 그린인프라 적용 : 전산유체역학을 활용한 수치분석 -

백 승 헌
생태조경·지역시스템공학부
서울대학교 대학원

한국은 OECD 회원국 중 대기오염이 심각한 국가 중 하나이다. 한국 내에서도 항만지역의 경우 많은 해양 물동량으로 인해 다량의 오염물질이 배출되고 있으며, 이는 해당 지역의 대기오염의 주 원인으로 높은 비중을 차지하고 있다. 현재 국내의 대기질 개선을 위한 정책으로는 배출원 자체만을 규제하는 정책이 주를 이루고 있다. 하지만 국내 주요 도시의 미세먼지 농도의 변동 추이를 살펴보았을 때, 배출원 규제 위주 정책의 효용성이 의문시되고 있으며 보다 공간적인 측면에서의 관리 방안이 필요함을 시사하고 있다.

본 연구는 한국의 항만도시 중 규모가 가장 큰 부산의 절반 이상의 해상 물동량을 처리하여 대기질이 좋지 않을 것으로 판단되는 부산신항을 대상으로 하였다. 더 세부적으로는, 부산신항 내에서도 인구가 밀집되어 있는 배후 주거단지를 대상으로 연구를 진행하였다. 부산신항 지역의 대기질 개선을 위해 기존의 배출원만을 규제하는 방법에서 벗어나 공간적 측면에서의 대응 방안이 필요하다고 판단하였다. 본 연구에서는 그 대응 방안으로 다양한 재난재해를 저감해주는 것으로 알려져있는 그린인

프라스트럭처를 활용하였다.

본 연구의 목적은 항만지역 배후 주거단지의 대기질을 개선하기 위해서 그린인프라스트럭쳐를 도입하였을 때, 정량적으로 얼마 만큼의 효과가 있는지 제시하고 나아가 그린인프라의 최적 배치안을 제시하는 것이다. 본 연구의 목적을 달성하기 위해서 대상지에 다양한 형태로 그린인프라스트럭처를 모의할 수 있고 그 효과를 정량적으로 나타낼 수 있는 전산유체역학을 활용하였다. CFD 모델을 활용하기 위해 미세먼지 관측소, 기상정보 데이터 등 현장 데이터와 상관성 분석을 진행하였으며, 결정계수 값이 0.7 이상으로 준수한 상관성을 보였다. 연구에 활용된 그린인프라스트럭처는 대상지역의 식재형태를 고려하여 교목과 관목을 활용하였고 식재 간격, 식재 배열을 조합하여 총 30개의 케이스에 대해 시뮬레이션하였다.

본 연구는 미세먼지 오염농도가 높지만 관리방안이 부족한 항만지역의 배후 주거단지에 대해 공간적 측면에서 개선 방안으로 그린인프라를 도입하였으며, 나아가 배치 방법을 제시하였다. 추후 본 연구가 항만지역 대기질의 공간적 개선 방안의 기초자료가 될 수 있을 것으로 판단된다.

keywords : 전산유체역학, 그린인프라스트럭처, 대기질, 항만지역, 미세먼지

Student Number : 2021-20044

References

Brunekreef, B., & Holgate, S. T. (2002). Air pollution and health. The lancet, 360(9341), 1233-1242.

Buccolieri, R., Santiago, J. L., Rivas, E., & Sanchez, B. (2018). Review on urban tree modelling in CFD simulations: Aerodynamic, deposition and thermal effects. Urban Forestry & Urban Greening, 31, 212-220.

Gallagher, J., Baldauf, R., Fuller, C. H., Kumar, P., Gill, L. W., & McNabola, A. (2015). Passive methods for improving air quality in the built environment: A review of porous and solid barriers. Atmospheric environment, 120, 61-70.

Gromke, C., & Blocken, B. (2015). Influence of avenue-trees on air quality at the urban neighborhood scale. Part II: Traffic pollutant concentrations at pedestrian level. Environmental Pollution, 196, 176-184.

Hong, B., Lin, B., & Qin, H. (2017). Numerical investigation on the coupled effects of building-tree arrangements on fine particulate matter (PM2. 5) dispersion in housing blocks. Sustainable cities and society, 34, 358-370.

Jeanjean, A. P., Buccolieri, R., Eddy, J., Monks, P. S., & Leigh, R. J. (2017). Air quality affected by trees in real street canyons: The case of Marylebone neighbourhood in central London. Urban Forestry & Urban Greening, 22, 41-53.

Jeanjean, A. P., Hinchliffe, G., McMullan, W. A., Monks, P. S., & Leigh, R. J. (2015). A CFD study on the effectiveness of trees to disperse road traffic emissions at a city scale. Atmospheric Environment, 120, 1-14.

Jeanjean, A. P., Monks, P. S., & Leigh, R. J. (2016). Modelling the effectiveness of urban trees and grass on PM2. 5 reduction via dispersion and deposition at a city scale. Atmospheric Environment, 147, 1-10.

Kadaverugu, R., Sharma, A., Matli, C., & Biniwale, R. (2019). High resolution urban air quality modeling by coupling CFD and mesoscale models: A review. Asia-Pacific Journal of Atmospheric Sciences, 55(4), 539-556.

Nowak, D. J., Hirabayashi, S., Bodine, A., & Hoehn, R. (2013). Modeled PM2. 5 removal by trees in ten US cities and associated health effects. Environmental pollution, 178, 395-402.

Santiago, J. L., Borge, R., Martin, F., De La Paz, D., Martilli, A., Lumbreras, J., & Sanchez, B. (2017). Evaluation of a CFD-based approach to estimate pollutant distribution within a real urban canopy by means of passive samplers. Science of The Total Environment, 576, 46-58.

Santiago, J. L., Martín, F., & Martilli, A. (2013). A computational fluid dynamic modelling approach to assess the representativeness of urban monitoring stations. Science of the total environment, 454, 61-72.

Toparlar, Y., Blocken, B., Maiheu, B., & Van Heijst, G. J. F. (2017). A review on the CFD analysis of urban microclimate. Renewable and Sustainable Energy Reviews, 80, 1613-1640.

Vos, P. E., Maiheu, B., Vankerkom, J., & Janssen, S. (2013). Improving local air quality in cities: to tree or not to tree?. Environmental pollution, 183, 113-122.

Vranckx, S., Vos, P., Maiheu, B., & Janssen, S. (2015). Impact of trees on pollutant dispersion in street canyons: A numerical study of the annual average effects in Antwerp, Belgium. Science of the Total Environment, 532, 474-483.

Zhong, M., Saikawa, E., Liu, Y., Naik, V., Horowitz, L. W., Takigawa, M., ... & Stone, E. A. (2016). Air quality modeling with WRF-Chem v3. 5 in East Asia: sensitivity to emissions and evaluation of simulated air quality. Geoscientific Model Development, 9(3), 1201-1218.
Zhong, M., Saikawa, E., Liu, Y., Naik, V., Horowitz, L. W., Takigawa, M., … & Stone, E. A. (2016). Air quality modeling with WRF-Chem v3. 5 in East Asia: sensitivity to emissions and evaluation of simulated air quality. Geoscientific Model Development, 9(3), 1201-1218.
한승재. (2020). 부산신항 선박 배출량 산정 및 주변지역 미세먼지 농도에 미치는 영향 분석.

해양수산부. (2021). 항만지역 등 대기질 개선 종합계획.